On Explaining the Tension in the Observations of the Hubble Parameter by the wLTB model

Master's Thesis

By:

BSc. Linda Cilla Emilia Tenhu

Supervisor:

Prof. Kimmo Kainulainen

JYVÄSKYLÄN YLIOPISTO
UNIVERSITY OF JYVÄSKYLÄ

Department of Physics

Jyväskylä 23.10.2018

Acknowledgements

I would first like to thank my supervisor Professor Kimmo Kainulainen of the Physics Department at University of Jyväskylä. He introduced me to the fascinating world of science by letting me in to the cosmology group and giving me the possibility to attend a cosmology conference. These opportunities, especially, gave me motivation for writing and finishing this thesis. And of course, help was always provided whenever I needed it.

I would also like to thank Assistant Professor Valerio Marra of the Federal University of Espírito Santo (UFES), Vitória, Brazil who gave us the idea of applying the wLTB model to the Hubble tension problem. Without his ideas, this thesis would have been totally different.

In addition, I would like to acknowledge Professor Kari J. Eskola of the Physics Department at University of Jyväskylä as the second reader of this thesis, and I am grateful to him for his perceptive comments.

Lastly, I must express my gratitude to my family and friends for providing me with valuable support and encouragement. This accomplishment would not have been possible without them. Thank you.

Abstract

Tenhu Linda Cilla Emilia
On Explaining the Tension in the Hubble Parameter Observations by the wLTB model
Master's Thesis
Department of Physics, University of Jyväskylä, 2018,

A tension of 3.6 standard deviation has been observed between the local (distance ladder) and global (cosmic microwave background) measurements in the expansion rate of the universe i.e. the present-day Hubble parameter value H_0. In this Master's Thesis, depart from the Standard Model of Cosmology, an inhomogeneous cosmological wLTB model is introduced to explain the observed tension. The wLTB model enables one to solve the Einstein's field equations exactly in an inhomogeneous but spherically symmetric case. This makes it possible to determine the current Hubble parameter value inside an inhomogeneous area called LTB bubble. It turns out that an underdense bubble increases the local Hubble parameter value and thus makes the wLTB model a possible candidate that can explain the Hubble parameter tension. However, arbitrary inhomogeneities as well as observer's arbitrary locations inside the bubble are not allowed. In the future, the challenge is to fit the restrictions for the inhomogeneity and the Hubble parameter observational data together.

Keywords: Inhomogeneous Cosmological Models, Hubble Parameter

Tiivistelmä

Tenhu Linda Cilla Emilia
Hubblen parametrin mittauksissa havaitun eron selittäminen wLTB -mallin avulla
Pro gradu -tutkielma
Fysiikan laitos, Jyväskylän yliopisto, 2018,

Tällä hetkellä universumin laajenemisnopeudessa eli Hubblen parametrin arvossa on havaittu noin 3,6 standardipoikkeaman ero paikallisen (etäisyystikapuut) sekä globaalin (kosminen taustasäteily) mittaustavan välillä. Tässä pro gradu -tutkielmassa esitetään kosmologisesta standardimallista poiketen epähomogeeninen wLTB-malli, jonka avulla kyseistä eroa voidaan selittää. wLTB-mallissa pystytään ratkaisemaan Einsteinin kenttäyhtälöt eksaktisti epähomogeenisessa pallosymmetrisessä tapauksessa, mikä mahdollistaa paikasta riippuvan Hubblen parametrin arvon määrittämisen epähomogeenisen alueen, eli LTB-kuplan sisällä. Osoittautuu, että ympäristöään harvempi kupla kasvattaa paikallista Hubblen vakion arvoa ja voi siten selittää eroa havaintojen välillä. Mielivaltainen epähomogenia eikä mielivaltainen havainnoijan sijainti epähomogenian sisällä ole kuitenkaan sallittu. Tulevaisuuden haasteena on sovittaa homogeniaan kohdistuvat rajoitukset yhteen havaitun Hubblen vakion poikkeaman kanssa.

Avainsanat: Epähomogeeniset kosmologiset mallit, Hubblen parametri

Contents

1 Introduction

During the first half of the 20th century theorists like A. Friedmann [1] (English translation [2]) had discovered that the universe might be expanding. After some observational evidence many physicists including A. G. Lemaître concluded [3] (English translation [4]) that the universe we live in is expanding. Since then scientists have been interested to determine the current value of the expansion rate of the universe, called the Hubble parameter. In the current light, the first determinations of the Hubble parameter using supernovae by Lemaître [3] and E. Hubble [5] were ambitious but not very succesful exceeding the most recent values by an order of magnitude. Later, especially closer to the end of the 20th century, the measurements got more and more accurate and seemed to agree around the value of 70 km/s/Mpc.

After the Cosmic Microwave Background (CMB) radiation was discovered in 1960's [6, 7], scientists figured out that the expansion rate could also be determined indirectly from the microwave background radiation. This gave the physics and astronomy community the possibility to compare the two independently determined values to each other.

Until the beginning of the 2010's these two ways to determine the current Hubble parameter value seemed to agree. Problems arose when the measurements got even more precise revealing that the local supernova data based measurements were invariably giving larger values than the global CMB based measurements. The trend of measurements over the last 17 years is illustrated in the Figure 1.1.

The tension between the Hubble parameter measurements has grown during the last few years, becoming as large as 3.6σ. This value is calculated from the most recent values [12] and [20] published during this year (2018) and is illustrated in the Figure 1.2.

Since this tension has not disappeared when the precision of the equipment and methods have increased, one has to look for other solutions, and so scientists have suggested many different approaches to this problem. The conservative approach

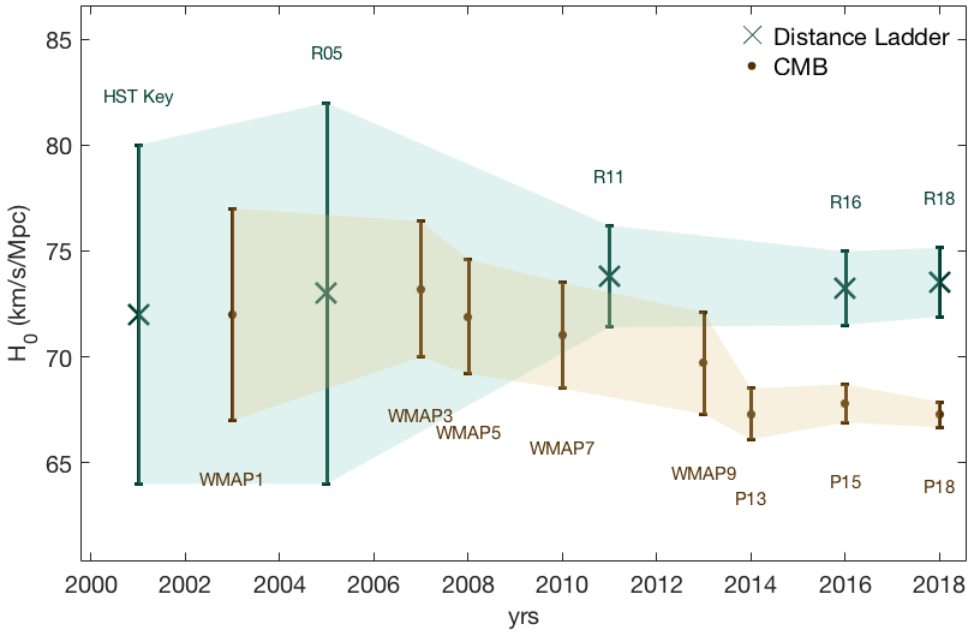

Figure 1.1. The Hubble parameter measurements over recent the years. When the measurements are getting more accurate the tension between the local (blue) [8, 9, 10, 11, 12] and global (yellow) [13, 14, 15, 16, 17, 18, 19, 20] measurements is clearly visible.

is that in one or both ways of measuring the Hubble parameter there occur some unknown systematics that cause the tension [21]. On the other hand, papers like [22] are calling for new physics. This can mean new neutrino physics [23], extended parameter space [24] or dark energy and modified gravity models [25], just to name a few attempts trying to alleviate the tension by the virtue of physics beyond the Standard Model of Cosmology. Yet, no one has really succeeded in discovering a widely accepted solution.

In this thesis a possible solution to explain the tension in the Hubble parameter measurements is introduced. An inhomogeneous but spherically symmetric model called wLTB model is suggested as a possible candidate that could explain the increased local Hubble parameter values.

In this model the Cosmological Principle, the principle telling the universe to be homogeneous and isotropic on large enough scales, is relaxed by giving up the general homogeneity and isotropicity condition while restricting inhomogeneities to obey spherical symmetry. This means that the model allows local spherically symmetric inhomogeneities to exist which can affect the local Hubble parameter values. It is

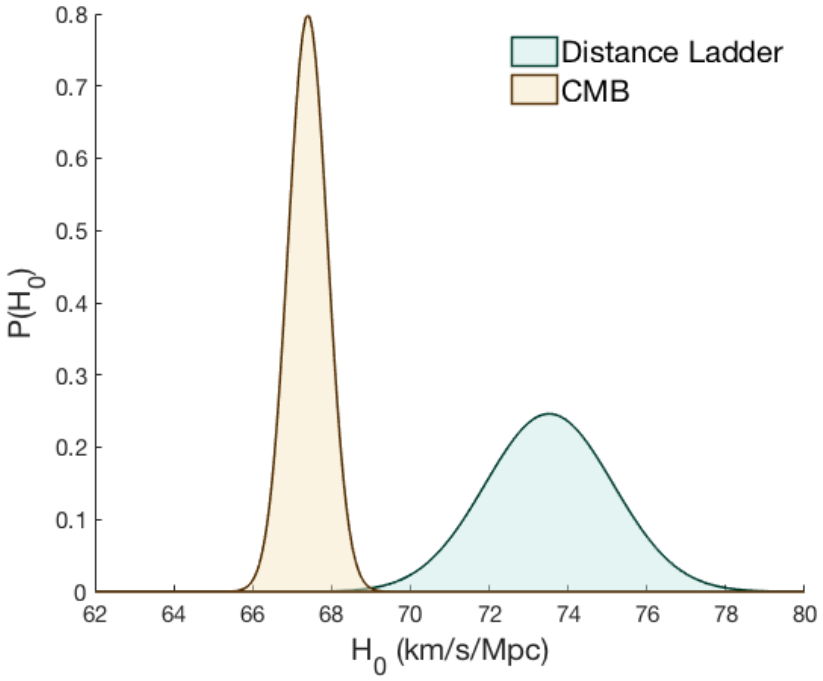

Figure 1.2. Comparison of the probability ditributions of the recent local (blue) [12] and global (yellow) [20] measurements for the current Hubble parameter value H_0. One can notice how only the tails of the distributions are touching yielding to a tension of 3.6σ.

assumed that a local underdensity would cause the local Hubble parameter value to increase and thus yield the observed tension. In addition, the dark energy equation of state parameter is not initially restricted to the value of $w_\Lambda = -1$ given by the Standard Model of Cosmology.

The importance of determining the current Hubble parameter value is clear when one wants to calculate for example the age of the universe which is inversely proportional to the present-day Hubble parameter value. Additionally, many other cosmological quantities such as the energy density of the universe is related to the Hubble parameter. Thus, during the era of precision cosmology, it is very important to be able to explain the tension and later settle on a well-agreed present-day Hubble parameter value.

In this thesis, basic properties of ΛCDM model, the Standard Model of Cosmology, are introduced in the section 2 followed by the section 3 discussing a reformulation of the Einstein's field equations called ADM formulation. This procedure is required for the section 4 where the inhomogeneous wLTB model is constructed. In the

section 5 preliminary results for the Hubble tension problem given by the wLTB model are introduced and a plan for upcoming statistical analysis is presented. In the end, the conclusions and outlook are discussed in the section 6.

2 ΛCDM model, The Standard Model of Cosmology

The simplest model that best agrees with cosmological observations is Big Bang Cosmology, which describes the origin of the universe as a singularity, a high-temperature and high-density state, following by an exponential expansion of space-time called inflation. After inflation the universe continued expanding, although not exponentially, and cooled down. This model can explain vast number of phenomena observed in the universe such as the Cosmic Microwave Background and Large-Scale Structure (LSS) formation.

The best parameterisation of the Big Bang Cosmology, according to the observations, is called ΛCDM, widely named as the Standard Model of Cosmology. The name of the parameterisation comes from the major components forming the energy density of the universe today. In ΛCDM the Greek letter Λ stands for the cosmological constant, the Dark Energy (DE) component, that plays the major role in the universe's energy density budget today, a bit less than 70 % and is thought to cause the observed accelerating expansion of the universe [26].

The other quite dominant constituent in the current energy density of the universe is called Cold Dark Matter (CDM). CDM is non-baryonic matter that is not visible through the photon channel. However, it is possible to observe the effects of CDM for example from the flat galaxy rotation curves. CDM is thought to interact with ordinary matter only by gravitational and possibly some new very weak force. Nowadays, the ΛCDM model states that CDM makes up $26-27\,\%$ of the universe's energy density. The remaining energy density is created by baryonic matter, about 5 %, and radiation, about 0.5 %, like the CMB radiation. [26]

The Standard Model of Cosmology assumes that on large enough scales the universe is spatially homogeneous and isotropic. This principle is called the Cosmological Principle. It tells that the location of Earth is not special and therefore one would get similar observational results in other locations in the universe, as well. In addi-

tion, the correct theory to describe gravitation is taken to be the general theory of relativity. [26]

In this chapter the properties and results of the Standard Model of Cosmology are discussed. Naturally, one starts from the spacetime metric and solutions for the Einstein's field equation.

2.1 Friedmann Equations

As is mentioned already, the Cosmological Principle states that the universe is spatially homogeneous and isotropic on large enough scales. Now, to describe the four-dimensional spacetime physically and, moreover, solve the Einstein's field equations, one has to formulate the spacetime metric describing the model under interest. The assumptions of the character of the spacetime given by ΛCDM yield to a metric of the form

$$\mathrm{d}s^2 = -\mathrm{d}t^2 + a^2(t)\mathrm{d}\sigma^2, \tag{2.1}$$

where $a(t)$ is a scale factor as a function of a timelike coordinate t. The scale factor measures the size of a three-dimensional spatial slice. The symbol $\mathrm{d}\sigma$ describes the line element on the three-dimensional spatial hypersurfaces and can be written as

$$\mathrm{d}\sigma^2 = h_{ij}(x)\mathrm{d}x^i\mathrm{d}x^j, \tag{2.2}$$

where h_{ij} is the three-dimensional metric and x^i are coordinates on the three-dimensional spatial slice. [27]

In order the three-dimensional spatial metric to obey the translational and rotational symmetry, the Cosmological Principle, the full four-dimensional line element takes the spherically symmetric form

$$\mathrm{d}s^2 = -\mathrm{d}t^2 + a^2(t)\left(\frac{\mathrm{d}r^2}{1-kr^2} + r^2\mathrm{d}\theta^2 + r^2\sin^2\theta\mathrm{d}\phi^2\right). \tag{2.3}$$

Here the symbol k describes the curvature of the spacetime. It is allowed to take the values of either $-1, 0$ or 1 describing the open, flat or closed universe, respectively,

when r is suitably normalised. The metric Eq. (2.3) ensures that the curvature of the four-dimensional spacetime is the same everywhere (possesses translational and rotational symmetry) at constant time and is widely called as the Friedmann-Lemaître-Robertson-Walker (FLRW) metric. [26]

The Einstein's field equations have to be considered if one wants to understand the behaviour of spacetime. Einstein himself wrote the equations into the form [28]

$$G_{\mu\nu} = \kappa T_{\mu\nu}, \tag{2.4}$$

where the Einstein tensor $G_{\mu\nu}$ can be expressed as a subtraction of the Ricci curvature scalar R from Ricci curvature tensor $R_{\mu\nu}$

$$G_{\mu\nu} = R_{\mu\nu} - \frac{1}{2}R, \tag{2.5}$$

where the proportionality constant $\kappa = 8\pi G$. Einstein's field equations tell how the spacetime metric and thus the curvature of the spacetime, responds to the energy and momentum in the spacetime, which is described by the energy-momentum tensor $T_{\mu\nu}$ [27].

In the Standard Model of Cosmology, the source for the energy and momentum is usually taken to be a perfect fluid. The characteristics of a perfect fluid can be described by an equation of state

$$p_i = w_i \rho_i, \tag{2.6}$$

where p_i stands for pressure and ρ_i the energy density of the fluid component i. The symbol w_i is called the equation of state parameter and it depends on the character of a particular fluid component. Different components of the fluid can represent different constituents of the universe, like matter or dark energy, all described by a unique equation of state.

As can be noticed from the above Eq. (2.6), perfect fluids do not have, a priori, any shear stresses, heat conduction or viscosity and the only thing needed to describe perfect fluids is the relation between pressure and energy density. In addition, perfect

fluids can be assumed to be at rest in comoving coordinates which means that the four velocity of a fluid component i reads

$$(U_\mu)_i = (1,0,0,0). \tag{2.7}$$

Now, one can write the energy-momentum tensor for a perfect fluid

$$T_{\mu\nu} = \sum_i \left[(\rho_i + p_i) (U_\mu)_i (U_\nu)_i + p_i g_{\mu\nu} \right], \tag{2.8}$$

where $g_{\mu\nu}$ is the four-dimensional spacetime metric. [27]

Now, all the required information at hand, one can plug the FLRW metric Eq. (2.3) as well as the energy-momentum tensor for the perfect fluid Eq. (2.8) to the Einstein's field equations Eq. (2.4) and get the Friedmann equation

$$H^2 = \left(\frac{a_{,t}}{a} \right)^2 = \frac{8\pi G}{3} \sum_i \rho_i \tag{2.9}$$

where the notation $,t$ stands for a time derivative and G the gravitational constant. In addition, the rate of change of the scale factor a is identified as the Hubble parameter H and the curvature is included as one of the energy density components

$$\rho_k = -\frac{3k}{8\pi G a^2}. \tag{2.10}$$

The second Friedmann equation can be derived from the spatial components of the Einstein field equation, Eq. (2.4), as well as using the first Friedmann equation, Eq. (2.9), to eliminate the first derivative of the scale factor. This gives

$$\frac{(a_{,t})_{,t}}{a} = -\frac{4\pi G}{3} \sum_i (\rho_i \ + 3p_i), \tag{2.11}$$

which is sometimes called an acceleration equation, as well. If one differentiates the first Friedmann equation Eq. (2.9) with respect to time and then substitutes it to the second equation Eq. (2.11) one gets the continuity equation for the energy

density

$$(\rho_i)_{,t} = -3H\,(\rho_i + p_i)\,. \tag{2.12}$$

2.2 The Hubble Parameter and the Expanding Universe

Georges Lemaître in 1927 [3] and then few years later Edwin Hubble [5] discovered that the further an object is located from us in the universe, the faster it moves away from us. This discovery has been called the Hubble law and its modern mathematical form reads

$$\mathbf{v}_p = H(t)\mathbf{s}_{pq}. \tag{2.13}$$

So to say, it describes the dependence of the recessional velocity $\mathbf{v}_p$ of an object p to the distance $\mathbf{s}_{pq}$ from the observer q to the object p. The proportionality constant is called the Hubble parameter which is a constant spatially but dynamical in time. The Hubble law is valid only on scales where the universe is homogeneous. [26]

The expansion of the universe can be demonstrated with an analogy of an expansion of a two-dimensional surface of a sphere of radius $R(t)$. As is shown in the Figure 2.1 one can see the proportionality between the angle θ_{pq} and the arc s_{pq} spanned by this angle. Mathematically this can be expressed as follows

$$s_{pq} = R(t)\theta_{pq}. \tag{2.14}$$

If the angle θ_{pq} is kept constant and the radius of the sphere is varied, the length of the arc changes, too. This is a direct analogy to the spacetime expansion of the universe. Additionally, one can also be interested in the rate of expansion i.e. how fast or slow the universe is expanding or shrinking, correspondingly. The time derivate of the Eq. (2.14) is of the form

$$(s_{pq})_{,t} = [R(t)]_{,t}\,\theta_{pq} \tag{2.15}$$

and if the equation Eq. (2.14) is solved for the angle θ_{pq} and substituted to the time

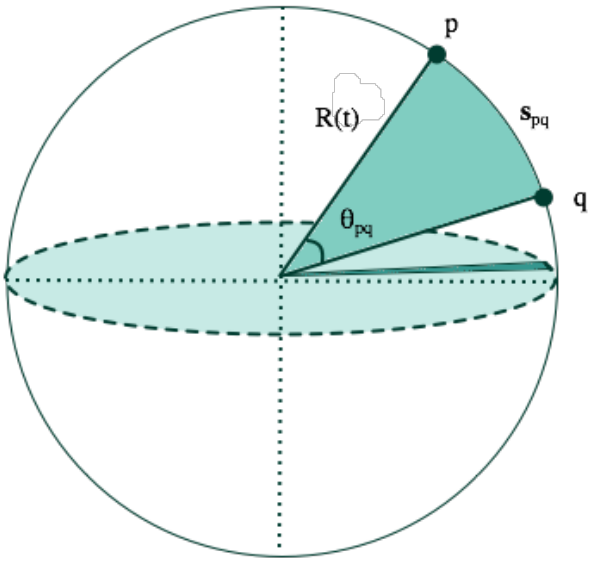

Figure 2.1. The properties of the arc lenght s_{pq} spanned by the angle θ_{pq} in a two-dimensional sphere of radius $R(t)$ can be used as an analogy when considering an expansion of a four-dimensional spacetime.

derivative Eq. (2.15) one can write

$$v_{pq} = \frac{[R(t)]_{,t}}{R(t)} s_{pq}. \tag{2.16}$$

In terms of the general convention, one uses normally a letter a to describe the distance scale and thus the Hubble parameter is defined as

$$H(t) = \frac{a_{,t}}{a} \tag{2.17}$$

and describes the rate of expansion of the universe where the symbol $a(t)$ is usually called the scale factor. [26]

A direct effect of the expansion of the universe is a phenomenon called cosmological redshift. This phenomenon can be observed as stretched wavelengths of light when photons have travelled through the expanding spacetime. More precisely, while light travels through the universe the spacetime expands and thus causes the wavelengths to get longer i.e. redder. This can be observed by comparing an absorption spectrum produced locally to an absorption spectrum produced by a distant light source where one can notice the increase in wavelength.

Mathematically, redshift is defined as

$$z = \frac{\lambda_{\text{obs}} - \lambda_{\text{em}}}{\lambda_{\text{em}}}, \tag{2.18}$$

where λ_{obs} is the observed wavelength and λ_{em} is the emitted wavelenght at the moment of emission. Redshift is also related to the scale factor as follows

$$1 + z = \frac{a_{\text{obs}}}{a_{\text{em}}}, \tag{2.19}$$

since the wavelegth is directly proportional to the scale factor. [26]

Redshift is one of the cosmological quantities that can be observed experimentally. Thus, the majority of the other cosmological parameters have to be written in terms of redshift or other cosmologically observable parameters. In the next section, this issue and how the Hubble parameter can be determined from observational data are discussed.

2.3 Hubble Parameter Measurements

When the Hubble law, the Eq. (2.13), is considered one notices that only two quantities, recessional velocity and disctance, have to be measured to get an experimental value for the Hubble parameter. The recessional velocity can be measured accurately from the redshift of the distant object in question. For small redshifts i.e. local objects, the recessional velocity and redshift are linearly proportional

$$v = cz. \tag{2.20}$$

For larger redshifts the relation is no longer linear and the matter-energy content of the universe has to be taken into account.

The main source of inaccuracy in the Hubble parameter measurements is the determination of the distance. The theory of cosmic distances and measurements of the distance to an object as well as Hubble parameter measurements from the Cosmic Microwave Background radiation data are discussed in the following sections.

2.3.1 Local Measurements i.e. the Distance Ladder

Cosmic distance measurements are tricky since distance itself is not a cosmic observable. Instead of distance, one is able to measure, for example, apparent magnitude or apparent luminosity of an object. In principle, if one knows that certain objects are radiating photons always with the same brightness one is able to compare the apparent luminosity of a nearby object, whose absolute luminosity and distance are known, to the apparent luminosities of similar objects further away and thus get an estimation for the distance of those further away objects. The comparison between the distances and luminosities can be done since, generally, the apparent luminosity of an object is inversely proportional to the square of the distance and therefore the more distant objects seem to be fainter.

As described above, the cosmic distances are measured in many parts by comparing objects' properties to each other and thus the cosmic distance measurements form a Cosmic Distance Ladder. In the following, this process in described in more detail.

The objects used for cosmic distance measurements have to have either the same brightness (or brightness that can be easily calibrated) or the same size so that after the comparison one can deduce something about their distance. Naturally, the objects have to be luminous enough that one can detect them from Earth. In addition, they have to have a characteristic property so that astronomers can distinguish them from all other bright objects in the universe. As a matter of fact, there exists several such objects and, in general, they are called standard candles or standard rulers. For example, Cepheid variable stars and Type Ia Supernovae (Ia SNe) are the most widely used standard candles, nowadays.

The Cepheid variable stars are massive stars which are burning helium and are about one thousand times more luminous than the Sun. The characteristic property of the Cepheid variable stars is their periodic pulsing rate. The pulsating period differs from about one to fifty days and is related to the brightness of the star. In general, the more luminous Cepheids pulse at a longer period. This period-luminosity relation, first found by Leavitt [29], can be used to determine the distances to far-off galaxies. [30]

The other example of a standard candle is the class of supernovae called Type Ia. Generally speaking, relatively massive stars end up as supernovae in the final steps of their stellar evolution. This means that they are exploding and spreading their

masses to the surroundings while exceeding the luminosity level of an average galaxy. [31]

Supernovae are categorised into two classes, Type II and Type I, depending on whether their spectra contain hydrogen or not, respectively. Further, Type I supernovae are categorised into three classes, a, b and c, determining is there silicon in the spectra (a) or not and how much helium it contains (b and c). [31]

In cosmic distance measurements the Type Ia supernovae are used because they are notably more luminous than the Type II supernovae and, moreover, the Type Ia supernovae have universally about the same mass and thus same luminosity. This consistency in the luminosity comes from the origin of the Type Ia supernovae. A Type Ia supernova is the final state of a white dwarf star located in a binary system and having mass comparable to the mass of the Sun $M_\odot$. These white dwarfs are constantly gaining mass from the other party of the binary system and, eventually, when exceeding the mass of $\sim 1.4M_\odot$ they collapse and form a supernova explosion. [31]

What makes the Type Ia supernovae highly suitable for the cosmic distance measurements is the fact that white dwarfs in general are not allowed to have mass larger than $\sim 1.4M_\odot$. This restriction comes from the Chandrasekhar limit which corresponds to the maximum mass of a star that can be stabilised by the quantum mechanical electron gas pressure which stems from the Pauli exclusion principle i.e. two fermions cannot occupy the same state. When the total mass accreted by the white dwarf in a binary system reaches the Chandrasekhar limit, it starts burn carbon and oxygen into heavier elements. This reaction releases enough energy for the whole system to be blown apart and form the Type Ia supernova [30]. The Chandrasekhar limit is assumed to be nearly universal so wherever the Type Ia supernovae are located, they are going through similar evolution and thus have about the same luminosity. [27]

By now it is clear that the apparent luminosity of a distant object has to be measured when trying to get an estimation for the distance to that object and, in the end, to be able get an experimental result for the current Hubble parameter value. The apparent luminosity i.e. the radiated flux density per unit area is defined as

$$F = \frac{L}{4\pi r^2}, \tag{2.21}$$

where L is the absolute luminosity of the object in question and the radius r forms the spherical surface through which the flux is determined i.e. the distance to the observer.

However, several issues have to be taken into account before one can reliably calculate distances from apparent luminosities. First, in order to be able to determine the flux density one has to know the absolute luminosity of an object. This is assumed to be possible by knowing the characteristic properties of the standard candles discussed earlier. Second, the universe is not a three-dimensional Euclidean space but four-dimensional spacetime with curvature properties so one has to be careful what it comes to the distance definitions. In addition, the expansion of the spacetime affects the photon wavelength and emission frequency causing them to get redshifted. [27]

To begin with, one can first consider the distance travelled by light during a time interval $t_0 - t$ where the zero denotes the current (later) time. The scale factor has evolved from $a(t)$ to $a(t_0)$ and therefore the horizon distance can be written as

$$d_H(t) = a(t_0) \int_t^{t_0} \frac{\mathrm{d}t}{a(t)}. \tag{2.22}$$

Instead of time, redshift is a cosmic observable and therefore one can perform variable changes to get

$$d_H(z) = \int_0^z \frac{\mathrm{d}z}{H(z)}. \tag{2.23}$$

To be able to write the Hubble parameter, Eq. (2.17), generally and in terms of redshift one has to consider the energy content of the universe. As was already mentioned, the universe can possess a certain geometry which is related to the curvature. Because the matter-energy curves the universe one can define the density parameter

$$\Omega = \frac{\rho}{\rho_c}, \tag{2.24}$$

where ρ_c denotes the critical density meaning the energy density required to make the universe exactly flat. So, if the total energy density of the universe ρ is larger

than the critical density the universe is positively curved. In turn, the smaller total energy density yields a negatively curved universe.

Today, the total energy density of the universe is observed to be very close to the critical density, corresponding to flat universe $k = 0$. From Eq. (2.9), it can be seen that the critical energy density and Hubble parameter are related by

$$H_0^2 = \frac{8\pi G}{3}\rho_c. \tag{2.25}$$

Dividing the Eq. (2.9) by the Eq. (2.25) one gets the relation

$$\frac{H^2}{H_0^2} = \sum_i \frac{\rho_i}{\rho_c}. \tag{2.26}$$

This expression can be related to the redshift by solving the continuity equation Eq. (2.12) yielding a relation between the energy density and scale factor

$$\rho_i \propto a^{-3(1+w_i)}. \tag{2.27}$$

Since the energy density is related to the scale factor by the Eq. (2.27) and to the critical density by the Eq. (2.24) as well as the the scale factor being related to redshift by the Eq. (2.19) one can formulate the Eq. (2.26)

$$H^2(z) = H_0^2 \sum_i \left[(\Omega_0)_i \, (1+z)^{3(1+w_i)} \right]. \tag{2.28}$$

This expression can now be substituted into the horizon distance formula, the Eq. (2.23), to get the horizon distance in terms of redshift and the current density parameter values:

$$d_H(z) = \frac{1}{H_0} \int_0^z \frac{\mathrm{d}z}{\sqrt{\sum_i \left[(\Omega_0)_i \, (1+z)^{3(1+w_i)} \right]}}. \tag{2.29}$$

The horizon distance measures the distance traveled by light on the spacetime manifold between observer and the light emitter. The relation between the horizon distance and the current Hubble parameter value H_0 is clear in the Eq. (2.29) yet

one can not use this distance measure directly in the flux density, Eq. (2.21), since it does not measure the angular distance.

The angular distance, say d_A, to an object of size s in Euclidean space is defined before, see the Eq. (2.14) and the Figure 2.1. Similarly, in a four-dimensional space-time, according to the FLRW metric, Eq. (2.3), the proper distance corresponding to angular separation $\mathrm{d}\theta$ with $\mathrm{d}t \equiv \mathrm{d}r \equiv \mathrm{d}\phi \equiv 0$ is

$$\mathrm{d}s^2 = a(t)^2 r^2 \mathrm{d}\theta^2. \tag{2.30}$$

Combining these two expressions, Eq. (2.14) and Eq. (2.30), gives for the angular distance

$$d_A = a(t)r. \tag{2.31}$$

Now, if one considers the radial distance travelled by light one gets, setting $\mathrm{d}s \equiv 0$ and $\mathrm{d}\theta = \mathrm{d}\phi = 0$ in the FLRW metric Eq. (2.3),

$$\int_t^{t_0} \frac{\mathrm{d}t}{a(t)} = \int_0^r \frac{\mathrm{d}r^2}{\sqrt{1-kr^2}}, \tag{2.32}$$

where one can identify the left hand side as the horizon distance Eq. (2.22) divided by the scale factor today. For the right hand side one can calculate analytically

$$\int_0^r \frac{\mathrm{d}r^2}{\sqrt{1-kr^2}} = \begin{cases} \arcsin r, & \text{if } k = -1 \\ r, & \text{if } k = 0 \\ \operatorname{arcsinh} r, & \text{if } k = +1, \end{cases} \tag{2.33}$$

where the different cases can be noted by a symbol $S_k(r)$ usually called generalized sine. Now, the equation Eq. (2.32) can be formulated as

$$\frac{d_H}{a(t_0)} = S_k(r). \tag{2.34}$$

Taking an inverse of the Eq. (2.34) gives the coordinate distance r. Substituting

this to the angular distance formula Eq. (2.31) yields

$$d_A(z) = \frac{1}{1+z_1} S_k^{-1}\left(\frac{d_H}{a(z_0)}\right), \tag{2.35}$$

where the $(1+z_1)^{-1} = a(z_1)$ is either the redshift at the moment of emission or absorption of photons, depending whether one observes standard candles or rulers. [27]

Before one plugs the angular distance, Eq. (2.35), in the formula for the apparent luminosity, Eq. (2.21), one has to consider the effects of expansion to the observed luminosity. The expansion of spacetime stretches the wavelengths of the photons so that their energy gets redshifted by a factor of $1+z$. Additionally, when the photons are being emitted the time interval gets redshifted which is thus affecting to their frequency by another factor of $1+z$. Since the apparent luminosity is defined

$$F = \frac{\text{number of photons observed}}{\text{area} \cdot \text{time}} \cdot \text{average energy}, \tag{2.36}$$

one notices that the observed luminosity gets the factor $(1+z)^{-2}$ by the effect of the expansion of spacetime. This factor can be absorbed to the definition of the luminosity distance yielding (standard candles: $z_1 = z$)

$$d_L(z) = (1+z) S_k^{-1}\left(\frac{d_H}{a(z_0)}\right), \tag{2.37}$$

so for the observed luminosity

$$F = \frac{L}{4\pi d_L^2}. \tag{2.38}$$

Instead of the apparent luminosities astronomers are observing the apparent magnitudes. The magnitudes are related to the observed flux densities as follows

$$m = -2.5 \log \frac{F}{F_0}, \tag{2.39}$$

where F_0 is some reference value. Naturally, the distances of different luminous

objects vary so the absolute magnitudes are different than the magnitudes observed from Earth. One can thus define a distance modulus as a subtraction of the absolute magnitude from the apparent magnitude

$$m - M = 5 \log \frac{d_L}{10\text{pc}}. \tag{2.40}$$

The relation to the luminosity distance is clear. [31]

In the next section, the focus is turned from the local measurements to the global ones. It turns out that the Cosmic Microwave Background radiation offers relevant information to determine the Hubble parameter globally.

2.3.2 Measurements from the CMB

The origin of the Cosmic Microwave Background (CMB) lies in the hot past of the universe. The early universe contained hot ionised plasma made of photons, electrons and nuclei. The photons' energies were larger than the ionisation energies of atoms and thus prevented atoms from being formed. Additionally, interactions between photons and electrons created pressure gradients in the primordial plasma which were then opposed by the gravitational effects from inhomogeneities causing oscillations in the density fluctuations [32].

When the universe expanded it also cooled and therefore the photons were no longer able to stop nuclei and electrons to form atoms, allowing the recombination to happen. Since atoms were formed the number of electrons decreased and thus the photon electron interactions were suppressed. This yielded a phenomenon called decoupling when the photon mean free path reached the scale of the age of the universe, causing the universe to become transparent. [33]

Thus, the CMB photons give information about the density oscillations in plasma which occurred just before the decoupling. On Earth one can observe this after-glow of the early universe in every direction in the sky. The temperature of the photons, while they have travelled through the expanding spacetime to our location, has got redshifted from temperatures of about 3000 K to about 3 K. Indeed, when studying the CMB more precisely one notices that no temperature is the same everywhere but has anisotropies, in relative scale $\sim 10^{-5}$, which are due to aforementioned

oscillation. [33]

However, it is not possible to predict a temperature value on a certain spot on the CMB. Instead, one can construct a radiation angular power spectrum because the expectation values of the amounts of the anisotropies on different scales can be calculated [27]. The resulting spectrum contains acoustic peaks which are sensitive, and hence yield information of fluctuations in the energy density of the constituents of the universe at the time of recombination. The precise form of the peaks depend on a number of cosmological parameters, such as baryon density, dark matter and dark energy and the Hubble expansion rate today, which all have to be determined simultaneously from the data. [32]

2.4 ΛCDM Input Parameters

To be complete in discussing the Standard Model of Cosmology it is appropriate to introduce the input parameters describing the model. As was mentioned in the beginning of this section, the Standard Model of Cosmology is a parameterisation of the general Big Bang Cosmology. It turns out that only six parameters suffice to construct a universe that looks statistically like the universe we are living in. The rest of the cosmological quantities can then be derived from these half a dozen initially determined parameters. The most recent values for the six parameters are determined by the virtue of the Planck 2018 data [20] and are listed in the Table 2.1.

In the parameter list Table 2.1, the scalar spectrum power-law index n_s describes how density fluctuations in the primordial plasma vary with scale and thus influence the characteristic scales of structure formation. If the scalar spectral index is exactly one, all the variations are the same on all scales. [34]

The Thomson scattering optical depth due to reionization τ, in turn, is a measure of the line-of-sight free electron opacity to CMB radiation. In other words, it measures how much the primary CMB anisotropies are scattered by the reionised medium at low redshifts. If the optical depth is zero it means there is no reionization at all. Larger values of τ imply larger values for z_{reion} which means the star and galaxy formation taking place earlier. Reionization means the era after the Dark Ages when the radiation emitted by gradually forming stars and galaxies reionize the intergalactic gas.

Table 2.1. The six input parameters in ΛCDM, the Standard Model of Cosmology. The values are from the most recent Planck 2018 data [20]. The number after the value denotes 1σ confidence level.

Parameter defition		Determined value [20]
Physical baryon density	$\Omega_b h^2$	0.02237 ± 0.00015
Physical CDM density	$\Omega_c h^2$	0.1200 ± 0.0012
Scalar spectrum power-law index	n_s	0.9649 ± 0.0042
Reionization optical depth	τ	0.0544 ± 0.0073
Power spectrum amplitude	$\ln(10^{10} A_s)$	3.044 ± 0.014
Angular parameter	$100\theta_{\mathrm{mc}}$	1.04092 ± 0.00031

The amplitude A_s measures the amplitude of the initial power spectrum of density perturbations and the angle θ_{mc} is a measure of the sound horizon at last scattering. Here the sound horizon means the distance sound waves could have travelled in the time on the primordial plasma before recombination. The angle is defined as follows

$$\theta_{mc} = \frac{r_s}{d_{sls}} \tag{2.41}$$

where r_s is the comoving size of the sound horizon and the d_{sls} denotes the comoving distance to the surface of last scattering.

In addition to the six parameters listed in the Table 2.1, ΛCDM assumes flat universe $k = 0$ and the dark energy to be the cosmological constant Λ.

In this thesis these independent ΛCDM parameters are used to describe the background FLRW universe.

In the Standard Model of Cosmology it is assumed that the correct theory of gravity is the general theory of relativity. In the next section 3 one can dive into this theory, more precisely, the Einstein's field equations and their reformulation. This is required if one wants to construct the inhomogeneous wLTB model which is then done in the section 4.

3 On Einstein's Field Equations and How to Solve Them

Einstein's field equations describe the behaviour of spacetime. John A. Wheeler has used an instructive expression on describing the meaning of the Einstein's field equations [35]:

> 'Spacetime tells matter how to move; matter tells spacetime how to curve.'

As was already mentioned in the section 2.1 the Einstein equations are of the form

$$G_{\mu\nu} = R_{\mu\nu} - \frac{1}{2}Rg_{\mu\nu} = 8\pi T_{\mu\nu}. \tag{3.1}$$

The left hand side describes the geometry of spacetime and this information is included in the Einstein tensor $G_{\mu\nu}$. On the other hand, the right hand side of the equation contains the source of gravity i.e. the density of matter-energy $T_{\mu\nu}$. [36]

As the name is telling, the Einstein's field equations are not just a single equation but a set of 10 second order non-linear partial differential equations for the symmetric metric tensor field $g_{\mu\nu}$. Four of the equations are not independent because of the Bianchi identity, $\nabla_\mu G_{\mu\nu} = 0$, 'the automatic conservation of source' [36]. Hence, the set contains only six truly independent equations.

What is to be solved from Einstein's field equations? One does not have absolute position or time from which the time evolution can be determined. In general relativity, the task is to solve for the spacetime geometry and structure itself i.e. for the components of the metric tensor in four spacetime dimensions. An obvious issue arises here, how one can solve for a time evolution of the metric tensor when time is not uniquely defined. A solution for this problem will be discussed in the following sections.

3.1 ADM Formalism

Einstein's field equations, Eq. (3.1), are non-linear, second order partial differential equations of the spacetime metric. Their evolution in time is not obvious, because the division of the spacetime manifold to space and time is not unique. Fortunately, a formalism that is able do to this has been developed and is called ADM or $3+1$ formalism after the developers Arnowitt, Deser and Misner, [37]. This formalism provides a tool, called spacetime foliation where the four-dimensional spacetime is foliated into three-dimensional spatial slices and one dimensional time, which allows general relativistic problems to be formulated in an initial value form. Also, the foliation allows us to visualize the general relativistic time evolution, see for example the Figure 3.1.

Spacetime is now constructed from three-dimensional constant time slices. All the quantities except time has to be specified on the three-dimensional spatial slices. This means that, somehow, one has to include all the four-dimensional information within three-dimensional quantities. Hence, new objects have to be introduced. First, the foliation parameters determining the way spacetime is foliated can be defined.

The basis of general relativity is a topological space called manifold. Generally, a manifold of dimension n can be considered to look locally like n-dimensional Euclidean space [27]. The global properties, in turn, can differ and concepts like curvature can be included. In general relativity, when speaking about the spacetime foliation one means that the four-dimensional manifold, the spacetime, is divided into three-dimensional hypersurfaces. [38]

Generally speaking, a hypersurface is an $(n-1)$-dimensional submanifold of the original n-dimensional manifold. One can define an induced metric on the hypersurface by the virtue of the four-dimensional metric of the whole manifold and normal vectors as follows

$$h_{\mu\nu} = g_{\mu\nu} + n_\mu n_\nu. \tag{3.2}$$

Here $g_{\mu\nu}$ is the full metric of the whole manifold whereas n^μ is the normal vector to a hypersurface. The induced metric $h_{\mu\nu}$ projects all the information along the normal vector field to the hypersurface and is thus a spatial quantity. [38]

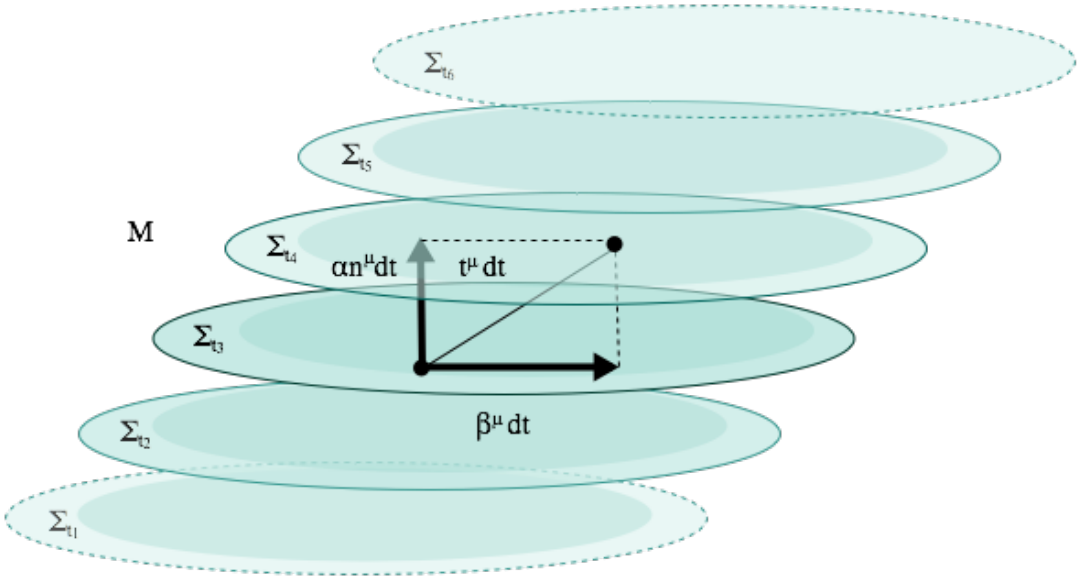

Figure 3.1. A manifold M is carved into hypersurfaces Σ_{t_n}. Notice the time flow vector field t^μ which has been divided into normal and tangential components. The normal component α is called lapse function and the tangetial one shift vector β^μ.

In the case of the general relativistic foliation, the hypersurfaces are non-intersecting, three-dimensional spatial slices each constant at time. The foliation style of the manifold can be determined by the foliation parameters. This can be done by dividing the time flow vector field, say t^μ, into normal and tangential parts,

$$t^\mu = \alpha n^\mu + \beta^\mu, \tag{3.3}$$

where $\alpha = -t^\mu n_\mu$ describes the elapsed time between the different hypersurfaces and is therefore called the lapse function. On the other hand, the tangential part which obeys $\beta^\mu n_\mu = 0$ can be written as

$$\beta_\mu = h_{\mu\nu} t^\nu, \tag{3.4}$$

where β_μ is called the shift vector which describes how much the spatial coordinates are shifted between the different hypersurfaces. For visualising the foliation and all the quantities related to it see the Figure 3.1. [39]

Since the four-dimensional spacetime has been carved into spatial slices all the curvature quantities have to be written in terms of three-dimensional corresponding objects. It is intuitive, though, that some information is lost when one replaces four-dimensional objects with three-dimensional ones. In practice, the three-dimensional Riemann tensor on the hypersurface does contain all the information about the intrinsic curvature of the hypersurface but the information about how the hypersurface looks when embedded into a higher dimensional space, into the whole four-dimensional manifold, is lost. More information about the Riemann curvature tensor is given in the Appendix A. [38]

Fortunately, there is a way to include the lost information about the extrinsic curvature of the hypersurface to the formulation. One can study a normal vector of a hypersurface, more precisely, how the gradients of this normal vector behave when projected on the spatial slice [38]. Since the induced metric acts as a projection tensor projecting all timelike quantities to the spatial slice one can define the extrinsic curvature tensor as follows

$$K_{\mu\nu} = -\frac{1}{2}\mathcal{L}_n h_{\mu\nu}, \tag{3.5}$$

where $\mathcal{L}_n$ denotes differentiation along a vector field, in this case the normal vector field n^μ and is called Lie derivative. The Lie derivative compares changes of a tensor field along a vector field. The vector field generates diffeomorphisms on the manifold and thus allows one to compare values of the tensor field at different points by pulling the tensor back to a point under interest. For more on Lie Derivatives, see Appendix B. To put it in a nutshell, Eq. (3.5) tells how the intrinsic metric changes along the normal, e.g. from slice to slice.

Now, after defining the extrinsic curvature tensor, one notices that it is related to a time-like derivative of the spatial metric and therefore it can be considered to be the first time derivative of the spatial metric.

3.2 The Line Element

The general ADM line element i.e. the quantity determining the distance on a given manifold is of the form

$$\boxed{\mathrm{d}s^2 = -\alpha^2 \mathrm{d}t^2 + h_{ij}\left(\mathrm{d}x^i + \beta^i \mathrm{d}t\right)\left(\mathrm{d}x^j + \beta^j \mathrm{d}t\right).} \tag{3.6}$$

This definition can be enlightened by the following schematic example.

The distance between two points on a manifold can be determined by calculating the inner product

$$\mathrm{d}s^2 = g_{\mu\nu}\mathrm{d}x^\mu \mathrm{d}x^\mu. \tag{3.7}$$

If the manifold is foliated into separate space and time dimensions the line element can be written in terms of temporal and spatial distances separately $\mathrm{d}x^\mu = t^\mu \mathrm{d}t + \mathrm{d}x^i$ as is illustrated in the Figure 3.2. On the other hand, one can also write the line element in terms of the foliation parameters α and β^μ by using the separation of the time flow vector t^μ, Eq. (3.3)

$$\mathrm{d}x^\mu = \alpha n^\mu \mathrm{d}t + \left(\beta^i \mathrm{d}t + \mathrm{d}x^i\right)\delta_i{}^\mu. \tag{3.8}$$

Now, one can write the general ADM line element by substituting the Eq. (3.8) to the inner product Eq. (3.7) and noticing that because the normal vector n^μ is totally time-like its inner product with itself equals to -1.

Thus, the ADM line-element Eq. (3.6) can be thought to resemblance the Pythagorean theorem in four dimensions and therefore it is intuitively clear that it gives the invariant distance between two points on the manifold, as can be seen in the Figure 3.2.[38]

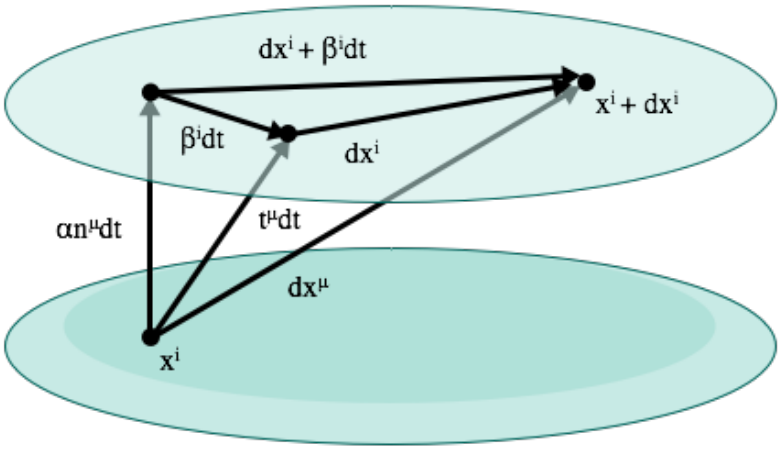

Figure 3.2. Schematical origin of the ADM line element Eq. (3.6). Starting from the inner product $\mathrm{d}s^2 = g_{\mu\nu}\mathrm{d}x^\mu \mathrm{d}x^\mu$ the line-element can be constructed by writing the $\mathrm{d}x$'s in terms of the foliation parameters.

3.3 General ADM Evolution Equations

In the ADM formulation of Einstein's field equations the dynamical variables which are to be evolved in time are the spatial metric and the extrinsic curvature $(h_{\mu\nu}, K_{\mu\nu})$. These parameters describe the state of the gravitational field at a certain time. One can then define the time evolution equations for these variables starting from the spatial metric.

The definition of the extrinsic curvature tensor, Eq. (3.5), directly gives Lie differentiation of the spatial metric along the normal vector field n^μ. To change the differentiation along the time flow vector field one can consider the Eq. (3.3) and expand the normal vector field as follows

$$K_{\mu\nu} = -\frac{1}{2\alpha}\left(\mathcal{L}_t h_{\mu\nu} - \mathcal{L}_\beta h_{\mu\nu}\right). \tag{3.9}$$

This procedure is legitimated by the linearity of Lie derivative, see the Appendix B, Eq. (B.6). Since the spatial metric does not have any temporal components its Lie derivative along the time flow vector reduces to a partial derivative having only spatial values that differ from zero. Similarly, due to the spatial character of the

shift vector the temporal components are zero and the indices can be replaced with spatial ones

$$-2\alpha K_{ij} = \partial_t h_{ij} - \mathcal{L}_\beta h_{ij}. \tag{3.10}$$

The Eq. (3.10) can be shortened by using a shorthand notation $^{\mathrm{d}}/_{\mathrm{d}t} = \partial_t - \mathcal{L}_\beta$ so the evolution equation for the spatial metric gets its general ADM form

$$\boxed{\frac{\mathrm{d}}{\mathrm{d}t} h_{ij} = -2\alpha K_{ij}.} \tag{3.11}$$

* * *

The evolution equation for the extrinsic curvature tensor can also be defined. Starting from the Lie derivative of the extrinsic curvature tensor along the time flow vector field

$$\mathcal{L}_t K_{\mu\nu} = \alpha \mathcal{L}_n K_{\mu\nu} + \mathcal{L}_\beta K_{\mu\nu}, \tag{3.12}$$

and applying the Ricci equation, see Appendix A, Eq. (A.11) to the first term on the right hand side one gets the expression

$$\mathcal{L}_t K_{\mu\nu} = \alpha \left(n^\delta n^\gamma h^\sigma{}_\mu h^\rho{}_\nu {}^{(4)}R_{\delta\rho\gamma\sigma} - \frac{1}{\alpha} D_\mu D_\nu \alpha - K^\gamma{}_\nu K_{\mu\gamma} \right) + \mathcal{L}_\beta K_{\mu\nu}. \tag{3.13}$$

Then, replacing the two normal vectors in the first term on the right hand side by the Eq. (3.2) yields

$$\begin{aligned} \mathcal{L}_t K_{\mu\nu} = &\alpha \left(h^{\gamma\delta} h^\sigma{}_\mu h^\rho{}_\nu {}^{(4)}R_{\delta\rho\gamma\sigma} - h^\sigma{}_\mu h^\rho{}_\nu {}^{(4)}R_{\rho\sigma} - \frac{1}{\alpha} D_\mu D_\nu \alpha - K^\gamma{}_\nu K_{\mu\gamma} \right) \\ &+ \mathcal{L}_\beta K_{\mu\nu}. \end{aligned} \tag{3.14}$$

The second term on the right hand side of the Eq. (3.14) can now be replaced by

use of the Einstein equation of the form [27]

$$^{(4)}R_{\mu\nu} = 8\pi G\left(T_{\mu\nu} - \frac{1}{2}Tg_{\mu\nu}\right) \tag{3.15}$$

and, in addition, the first term on the right hand side of the Eq. (3.14) can be changed by using the contracted Gauss equation, Appendix A, Eq. (A.7) as well as the symmetry of the two indices of the extrinsic curvature tensor as well as the Ricci tensor to get

$$\begin{aligned}\mathcal{L}_t K_{\mu\nu} = \alpha\Big(&R_{\mu\nu} + KK_{\mu\nu} - 2K^{\epsilon}{}_{\nu}K_{\epsilon\mu} - 8\pi G h^{\sigma}{}_{\mu}h^{\rho}{}_{\nu}\left(T_{\sigma\rho} - \frac{1}{2}Tg_{\sigma\rho}\right)\\ &-\frac{1}{\alpha}D_\mu D_\nu\alpha\Big) + \mathcal{L}_\beta K_{\mu\nu}.\end{aligned} \tag{3.16}$$

To simplify the evolution equation of the extrinsic curvature, the Eq. (3.16), several shorthand notations can be created:

$$\begin{aligned}S_{\mu\nu} &= h^{\rho}{}_{\mu}h^{\sigma}{}_{\nu}T_{\rho\sigma},\\ S &= S^{\mu}{}_{\mu},\\ \rho &= n^\mu n^\nu T_{\mu\nu}.\end{aligned} \tag{3.17}$$

Now, the Eq. (3.16) can be written as

$$\begin{aligned}\mathcal{L}_t K_{\mu\nu} = \alpha\left(R_{\mu\nu} + KK_{\mu\nu} - 2K^{\epsilon}{}_{\nu}K_{\epsilon\mu}\right) - \alpha 8\pi G\left(S_{\mu\nu} - \frac{1}{2}h_{\mu\nu}\left(S-\rho\right)\right)\\ - D_\mu D_\nu\alpha + \mathcal{L}_\beta K_{\mu\nu}.\end{aligned} \tag{3.18}$$

To shorten the evolution equation even more one can use one more shorthand notation

$$M_{\mu\nu} = S_{\mu\nu} - \frac{1}{2}h_{\mu\nu}\left(S-\rho\right) \tag{3.19}$$

to get

$$\mathcal{L}_t K_{\mu\nu} = \alpha \left(R_{\mu\nu} + K K_{\mu\nu} - 2K^{\epsilon}{}_{\nu} K_{\epsilon\mu} - 8\pi G M_{\mu\nu} \right) - D_\mu D_\nu \alpha + \mathcal{L}_\beta K_{\mu\nu}. \tag{3.20}$$

Also here the Lie derivative along the time coordinate reduces to a partial derivative and thus only spatial indices give non-trivial equations. As before, the partial and Lie derivatives of the extrinsic curvature tensor can be combined to form just one operator $^{\mathrm{d}}/_{\mathrm{d}t} = \partial_t - \mathcal{L}_\beta$ giving

$$\boxed{\frac{\mathrm{d}}{\mathrm{d}t} K_{ij} = \alpha \left(R_{ij} + K K_{ij} - 2K^{l}{}_{j} K_{li} - 8\pi G M_{ij} \right) - D_i D_j \alpha.} \tag{3.21}$$

The equation Eq. (3.21) can be called the evolution equation of the extrinsic curvature.

3.4 General ADM Constraint Equations

When solving a general relativistic problem constraint equations are solved on an initial spatial slice. Then they are evolved by the evolution equations to be sure that they will be satisfied also at later times. This yields a fact that the constraint equations do not contain any time derivatives but instead, they make sure that the Einstein's field equations will be solved on each slice. Thus, they provide initial value constraints for the system.

Hamiltonian constraint equation can be derived by considering the Einstein's field equations Eq. (3.1)

$$^{(4)}R_{\mu\nu} - \frac{1}{2} {}^{(4)}R g_{\mu\nu} = 8\pi G T_{\mu\nu}. \tag{3.22}$$

Here the numbers on the left hand side superscripts denote the dimensionality of the quantities. The Einstein's field equations can be multiplied by two normal vectors

$n^\alpha n^\beta$ and by a factor 2 to get

$$2{}^{(4)}R_{\mu\nu}n^\mu n^\nu - {}^{(4)}Rg_{\mu\nu}n^\mu n^\nu = 16\pi G\rho, \tag{3.23}$$

where a shorthand notation on the first row of Eq. (3.17) was used. Then, the left hand side of the equation Eq. (3.23) can be replaced with twice contracted Gauss equation, Appendix A Eq. (A.8), to get

$$\boxed{{}^{(3)}R + K^2 - K^{\mu\nu}K_{\mu\nu} = 16\pi G\rho.} \tag{3.24}$$

This equation is the Hamiltonian constraint equation.

* * *

The momentum constraint equation can also be derived from the Einstein's field equations multiplying them by the spatial metric $h^\alpha{}_\mu$ and the normal vector n^δ

$$h^\alpha{}_\mu n^{\delta\,(4)}R_{\alpha\delta} - \frac{1}{2}h^\alpha{}_\mu n^{\delta\,(4)}Rg_{\alpha\delta} = 8\pi G h^\alpha{}_\mu n^\delta T_{\alpha\delta}. \tag{3.25}$$

The second term on the right hand side is zero because of the inner product of the spatial metric and the normal vector. Equating the Eq. (3.25) and the contracted Codazzi equation, see Appendix A the Eq. (A.10) gives

$$D_\nu K_\mu{}^\rho - D_\mu K = -8\pi G h^\alpha{}_\mu n^\delta T_{\alpha\delta}. \tag{3.26}$$

The right hand side of the equation can be simplified by writing $S_\mu = -h^\alpha{}_\mu n^\delta T_{\alpha\delta}$ to get the momentum constraint equation

$$\boxed{D_\nu K_\mu{}^\rho - D_\mu K = 8\pi G S_\mu.} \tag{3.27}$$

The two ADM constraint equations Eq. (3.24), Eq. (3.27) and the two ADM evolution equations Eq. (3.11), Eq. (3.21) are equivalent to the Einstein's field equations.

Thus, one can solve the Einstein's field equations by giving sufficient initial conditions, namely data considering initial $h_{\mu\nu}$ and $K_{\mu\nu}$, that satisfy the ADM constraint equations. Then one can determine the state of the system at any point in spacetime by evolving the system in terms of the ADM evolution equations.

4 wLTB model, The Possible Solution

The standard model of cosmology, ΛCDM, assumes the cosmological principle to apply, which means the universe to be spatially homogeneous and isotropic. By now, various observations have shown existence of inhomogeneities such as voids [40], galaxy filaments [41] and superclusters [42] at least up to scale of order 100 Mpc. In addition, all the observations are made from the single point, from our location in the Solar System in Milky Way Galaxy and the Local Galaxy Group. There is no possibility to compare the results with others gotten from completely different locations. Hence, one does not know how much the inhomogeneities of the universe affect the observed values of the cosmological parameters. Consequently, it is useful to study what happens if the spatial homogeneity requirement is excluded. Thus, in this section, the focus is on an inhomogeneous but spherically symmetric cosmological model called Lemaitre-Tolman-Bondi (LTB) model. The LTB model is named after its developers, Lemaître [43], Tolman [44] and Bondi [45].

The wLTB model is the simplest inhomogeneous exact solution to the Einstein's field equations because it possesses spherical symmetry. The inhomogeneities are radial around the symmetry point which, in the simplest case, is the point of observation.

As is already mentioned earlier in the section 3, the dynamics of the spacetime is governed by the Einstein's field equations each of which contains a term that describes the energy-momentum of the spacetime. In cosmology, the energy-momentum can be expressed as a perfect fluid and therefore the constituents of the energy-momentum, like matter or dark energy, can be considered as different components of the resulting cosmic fluid. Each of these fluid components have their own equation of state, $p_i = w_i \rho_i$, which describes the relation of pressure and energy density.

The equation of state parameter w_Λ for the dark energy component is taken to be constant in the Standard Model of Cosmology and it is set to have a value of -1. Departing from the ΛCDM model, the dark energy equation of state parameter can also be allowed to vary or take another value. In this case, one can construct, for example, an inhomogeneous model where the dark energy equation of state

parameter has a value other than -1, i.e. the wLTB model.

4.1 ADM Equations in Spherical Symmetry

The ADM formalism can be used to construct an inhomogeneous LTB cosmology by including spherical symmetry in the general ADM equations derived in the section 3. Additionally, one has to formulate the equations governing the behaviour of the source terms, the cosmic fluid, as well as include the inhomogeneity. But first, one must specify the foliation parameters. The gauge choice determines how the information of the the field data flows through the time slices. The way of connecting the neighbouring time slices is related to the choice of the lapse function and thus determines the time slicing. On the other hand, the spatial gauge choice is related straightforwardly to the shift vector.

From now on, the foliation parameters are chosen so that the resulting coordinates will be the synchronous coordinates i.e. the coordinate time for all comoving observes is the proper time and the time coordinate is orthogonal to the spatial coordinates. This choice is called Geodesic slicing and it is the simplest choice because it sets the shift vector to zero and lapse function to unity:

$$\alpha = 1, \quad \beta^i = 0. \tag{4.1}$$

The name of the slicing comes from that fact that normal observes are freely falling and hence follow geodesics. [38]

For simplicity as well as for better numerical behaviour, a change of variables is performed and therefore the three-metric components are written as

$$\begin{aligned} h_{rr} \rightarrow \quad & H_{rr} \equiv \sqrt{h_{rr}} \\ h_{\theta\theta} \rightarrow \quad & H_{\theta\theta} \equiv \sqrt{h_{\theta\theta}}. \end{aligned} \tag{4.2}$$

The general ADM line element, Eq. (3.6), derived in the section 3.2 can be trans-

formed into a spherically symmetric form as follows

$$\mathrm{d}s^2 = -\mathrm{d}t^2 + h_{rr}\mathrm{d}r^2 + h_{\theta\theta}\left(\mathrm{d}\theta^2 + \sin^2\theta\mathrm{d}\phi^2\right). \tag{4.3}$$

It can be noticed that the foliation parameters are now specified in terms of the Geodesic Slicing, Eq. (4.1). Furthermore, taking the condition Eq. (4.2) into account the metric takes the form

$$\boxed{\mathrm{d}s^2 = -\mathrm{d}t^2 + H_{rr}^2\mathrm{d}r^2 + H_{\theta\theta}^2\left(\mathrm{d}\theta^2 + \sin^2\theta\mathrm{d}\phi^2\right).} \tag{4.4}$$

4.1.1 Evolution Equations

The corresponding spherically symmetric evolution equations for the metric components H_{ii} can be derived straightforwardly by remembering the general ADM form Eq. (3.11)

$$\boxed{H_{ii,t} = -H_{ii}K^i{}_i,} \tag{4.5}$$

where, for the sake of brevity, the partial derivative is written as a comma followed by the differentiation variable in the subscript. It can be noticed that the only independent equations are for the components H_{rr} and $H_{\theta\theta}$.

* * *

The evolution equations of the extrinsic curvature tensor can also be modified to the spherically symmetric form. Starting from the general ADM form Eq. (3.21) and again applying the Geodesic Slicing, Eq. (4.1), one gets

$$K_{ij,t} = {}^{(3)}R_{ij} - 2K^l{}_jK_{li} + KK_{ij} - \kappa M_{ij}, \tag{4.6}$$

where $\kappa = 8\pi G$. For simplicity, one can raise one index of the extrinsic curvature tensor which results in only two independent and non-zero components $K^r{}_r$ and $K^\theta{}_\theta$

due to the nature of the metric components, see the Eq. (4.4). So, the Eq. (4.6) with mixed indices is of the form

$$\partial_t \left(h_{ij} K^i{}_j \right) = h_{ij} \left({}^{(3)}R^i{}_j - 2K^{li}K_{li} + KK^i{}_j - \kappa M^i{}_j \right). \tag{4.7}$$

The indices can be raised by the spatial metric since the extrinsic curvature tensor is by definition purely spatial. Then, the left hand side of the Eq. (4.7) can be expanded and the general ADM metric evolution equation, the Eq. (3.11), substituted to get

$$-2K_{ij}K^i{}_j + h_{ij}K^i{}_{j,t} = h_{ij} \left({}^{(3)}R^i{}_j - 2K^{li}K_{li} + KK^i{}_j - \kappa M^i{}_j \right). \tag{4.8}$$

Because of the symmetry of the extrinsic curvature tensor as well as the freedom of renaming dummy indices one can write

$$h_{ij}K^i{}_{j,t} = h_{ij} \left({}^{(3)}R^i{}_j + KK^i{}_j - \kappa M^i{}_j \right). \tag{4.9}$$

Now, it is clear that the only completely independent and non-zero equations are

$$\begin{aligned} K^r{}_{r,t} &= {}^{(3)}R^r{}_r + K^r{}_r K^r{}_r + 2K^\theta{}_\theta K^r{}_r - \kappa M^r{}_r \\ K^\theta{}_{\theta,t} &= {}^{(3)}R^\theta{}_\theta + K^\theta{}_\theta K^r{}_r + 2K^\theta{}_\theta K^\theta{}_\theta - \kappa M^\theta{}_\theta . \end{aligned} \tag{4.10}$$

The next task is to calculate analytically the components of the three-dimensional Ricci tensor terms in the Eq. (4.10). To do this one has to expand the Ricci tensor by calculating the Christoffel connection coefficients related to the three-dimensional metric h_{ij} (see the corresponding definition in four dimensions: Eq. (A.2) introduced in the Appendix A). The non-zero Christoffel connection coefficients are

$$\begin{aligned} &{}^{(3)}\Gamma^r{}_{rr} = \frac{H_{rr,r}}{H_{rr}}, \quad {}^{(3)}\Gamma^r{}_{\theta\theta} = -\frac{H^2_{\theta\theta,r}}{2H^2_{rr}}, \quad {}^{(3)}\Gamma^r{}_{\phi\phi} = -\sin^2\theta \frac{H^2_{\theta\theta,r}}{2H^2_{rr}}, \\ &{}^{(3)}\Gamma^\theta{}_{r\theta} = \frac{H^2_{\theta\theta,r}}{2H^2_{\theta\theta}}, \quad {}^{(3)}\Gamma^\theta{}_{\phi\phi} = -\sin\theta\cos\theta, \\ &{}^{(3)}\Gamma^\phi{}_{r\phi} = \frac{H^2_{\theta\theta,r}}{2H^2_{\theta\theta}}, \quad {}^{(3)}\Gamma^\phi{}_{\theta\phi} = \frac{1}{\tan\theta}. \end{aligned} \tag{4.11}$$

The Ricci tensor is once contracted Riemann curvature tensor (see the four dimensional corresponding definition the Eq. (A.1))

$$ {}^{(3)}R_{ij} = {}^{(3)}\Gamma^{n}{}_{ij,n} - {}^{(3)}\Gamma^{n}{}_{in,j} + {}^{(3)}\Gamma^{n}{}_{nm}\,{}^{(3)}\Gamma^{m}{}_{ij} + {}^{(3)}\Gamma^{n}{}_{jm}\,{}^{(3)}\Gamma^{m}{}_{in}. \tag{4.12} $$

Substituting the non-zero connection coefficients Eq. (4.11) to the three-dimensional Ricci tensor Eq. (4.12) one gets the non-zero Ricci tensor components

$$ \begin{aligned} {}^{(3)}R_{rr} &= -\partial_r\left(\frac{H^2_{\theta\theta,r}}{H^2_{\theta\theta}}\right) + \frac{H_{rr,r}}{H_{rr}}\frac{H^2_{\theta\theta,r}}{H^2_{\theta\theta}} - \frac{1}{2}\left(\frac{H^2_{\theta\theta,r}}{H^2_{\theta\theta}}\right)^2 \\ {}^{(3)}R_{\theta\theta} &= -\frac{H^2_{\theta\theta,r}}{2H^2_{\theta\theta}} + 1 - \frac{H_{rr,r}}{H_{rr}}\frac{H^2_{\theta\theta,r}}{2H^2_{\theta\theta}} \\ {}^{(3)}R_{\phi\phi} &= \sin^2\theta\,{}^{(3)}R_{\theta\theta}. \end{aligned} \tag{4.13} $$

A shorthand notation

$$ X = \frac{H_{\theta\theta,r}}{H_{rr}} \tag{4.14} $$

can be used to write the non-trivial components of the Ricci tensor with mixed indices

$$ \begin{aligned} {}^{(3)}R^{r}{}_{r} &= -\frac{2X_{,r}}{H_{rr}H_{\theta\theta}} \\ {}^{(3)}R^{\theta}{}_{\theta} &= -\frac{X,r}{H_{rr}H_{\theta\theta}} + \frac{1-X^2}{H^2_{\theta\theta}} \\ {}^{(3)}R^{\phi}{}_{\phi} &= \sin^2\theta\,{}^{(3)}R^{\theta}{}_{\theta}. \end{aligned} \tag{4.15} $$

Finally, comparing the Eq. (4.10) and Eq. (4.15) one gets the spherically symmetric

evolution equations for the extrinsic curvature tensor with mixed indices

$$\boxed{\begin{aligned} K^{r}{}_{r,t} &= -\frac{2X_{,r}}{H_{rr}H_{\theta\theta}} + K^{r}{}_{r}K^{r}{}_{r} + 2K^{\theta}{}_{\theta}K^{r}{}_{r} - \kappa M^{r}{}_{r} \\ K^{\theta}{}_{\theta,t} &= -\frac{X,r}{H_{rr}H_{\theta\theta}} + \frac{1-X^2}{H^2_{\theta\theta}} + K^{\theta}{}_{\theta}K^{r}{}_{r} + 2K^{\theta}{}_{\theta}K^{\theta}{}_{\theta} - \kappa M^{\theta}{}_{\theta}\,. \end{aligned}} \tag{4.16}$$

4.1.2 Constraint Equations

In order to write the general ADM Hamiltonian constraint equation, the Eq. (3.24), in spherical symmetry, one can expand it by writing out the Einstein summation convention

$${}^{(3)}R^{r}{}_{r} + 2\,{}^{(3)}R^{\theta}{}_{\theta} + \left(K^{r}{}_{r} + 2K^{\theta}{}_{\theta}\right)^2 - \left(K^{r}{}_{r}\right)^2 - 2\left(K^{\theta}{}_{\theta}\right)^2 = 2\kappa\rho. \tag{4.17}$$

where $\kappa = 8\pi G$. Then, by substituting the non-vanishing Ricci tensor components Eq. (4.15) one gets

$$\boxed{-\frac{2X_{,r}}{H_{rr}H_{\theta\theta}} + \frac{1-X^2}{H^2_{\theta\theta}} + \left(K^{\theta}{}_{\theta}\right)^2 + 2K^{r}{}_{r}K^{\theta}{}_{\theta} = \kappa\rho} \tag{4.18}$$

which is the Hamiltonian constraint equation in spherical symmetry.

* * *

The general ADM form of the momentum constraint equation, the Eq. (3.27), can be turned into spherical symmetry by expanding the three-dimensional covariant derivative (see the definition in the Eq. (A.4))

$$K^{j}{}_{i,j} + \Gamma^{j}_{jn}K^{n}{}_{i} - \Gamma^{n}_{ji}K^{j}{}_{n} - K_{,i} = \kappa S_i, \tag{4.19}$$

where again $\kappa = 8\pi G$. Calculating the components $i = r$ and $i = \theta$ gives

$$\Gamma^r_{rr}K^r{}_r + \Gamma^\theta_{\theta r}K^r{}_r + \Gamma^\phi_{\phi r}K^r{}_r - \Gamma^r_{rr}K^r{}_r - \Gamma^\theta_{\theta r}K^\theta{}_\theta - \Gamma^\phi_{\phi r}K^\phi{}_\phi - 2K^\theta{}_{\theta,r} = \kappa S_r, \quad (4.20)$$

$$K^\theta{}_{\theta,\theta} + \Gamma^\phi_{\phi\theta}K^\theta{}_\theta - \Gamma^\phi_{\phi\theta}K^\phi{}_\phi - K^r{}_{r,\theta} - 2K^\theta{}_{\theta,\theta} = \kappa S_\theta, \quad (4.21)$$

where one can substitute the connection coefficients Eq. (4.11) and divide by -2 to get

$$\boxed{\frac{H_{\theta\theta,r}}{H_{\theta\theta}}\left(K^\theta{}_\theta - K^r{}_r\right) + K^\theta{}_{\theta,r} = -\frac{1}{2}\kappa S_r} \quad (4.22)$$

for the r component and zero for the angular component θ. So the Eq. (4.22) is the only non-trivial momentum constraint in spherical symmetry.

* * *

It turns out, that terms like

$$\frac{1 - X^2}{H^2_{\theta\theta}}, \quad (4.23)$$

while perfectly defined when r approaches to zero, do not behave very well there numerically. This is because the angular scale factor $H_{\theta\theta}$ is directly proportional to the radius r, and vanishes when r gets small. To obtain smooth behaviour, the extrinsic curvature tensor must approach unity to very high accuracy, which cannot be treated numerically. However, there is a solution to this problem, if one defines the radial scale function H_{rr} similarly as is done in [46]:

$$H_{rr} = \frac{H_{\theta\theta,r}}{\sqrt{1 + 2E}}, \quad (4.24)$$

which requires a new variable E. The variable E can be considered as a curvature function. Thus, remembering the shorthand notation Eq. (4.14) one can write the

problematic terms as follows

$$\frac{1-X^2}{H_{\theta\theta}^2} = -\frac{2E}{H_{\theta\theta}^2}. \tag{4.25}$$

Now, one expects that the curvature function E is proportional to the radius squared near $r \approx 0$ and the ratio appearing in Eq. (4.25) is numerically stable. Hence, some of the ADM equations can be rewritten by paying attention to the numerical stability. One can start from the metric evolution equation, which can be reformulated bu use of the momentum constraint equation Eq. (4.22) which yields

$$\boxed{E_{,t} = (1+2E)\frac{H_{\theta\theta}}{H_{\theta\theta,r}}\frac{\kappa}{2}S_r.} \tag{4.26}$$

In addition, the Hamiltonian constraint Eq. (4.18) can be re-expressed, too, which gives

$$\boxed{-\frac{2X_{,r}}{H_{rr}H_{\theta\theta}} - \frac{2E}{H_{\theta\theta}^2} + \left(K^{\theta}{}_{\theta}\right)^2 + 2K^{r}{}_{r}K^{\theta}{}_{\theta} = \kappa\rho.} \tag{4.27}$$

This form of the Hamiltonian constraint is used in this thesis.

4.2 Fluid equations: the Energy-Momentum

Up to this point, the focus has been mainly on the left hand side of the Einstein's field equations. In this section, instead, the main issue is to develop mathematical description for the behaviour of the right hand side of the Einstein's field equations, the source terms. As an example, one has to take care that the covariant conservation of the energy momentum is guaranteed in the system.

The energy-momentum tensor that describes all sources of energy-momentum in the universe, except gravity, has already appeared in the evolution equation of the extrinsic curvature Eq. (4.16) and in the Hamiltonian constraint equations Eq. (4.27) as well as in the momentum constraint equation Eq. (4.22) as a source. This means that one has to solve simultaneously the ADM equations and the conservation equations related to the energy-momentum to determine the entire foliation of the space-

time. This is because the source terms $\rho\,, S_i$ and S_{ij} are different projections of the energy-momentum tensor either onto the hypersurface or in the direction of the normal vector and thus have direct effect on the foliation. [38]

In this model, the source of "matter"-energy (all other sources but gravity) are described by a set of perfect fluids. In the section 2, the energy-momentum tensor for such a system was introduced, the Eq. (2.8):

$$T^{\mu\nu} = \sum_i \left[(\rho_i + p_i)u_i^\mu u_i^\nu + p_i g^{\mu\nu}\right]. \tag{4.28}$$

Here the time-like and unitary vector field u_i^μ is taken to be of the form

$$u_i^\mu = \left(\gamma_{v_i}, \frac{\gamma_{v_i} v_i}{H_{rr}}, 0, 0\right), \tag{4.29}$$

where v_i expresses the proper radial velocity and $\gamma_{v_i}^2 = {}^1\!/\!_{(1\,-\,v_i^2)}$ is the Lorenz gamma factor. In addition, the fluid is assumed to be multicomponental i.e the different components being the different sources of energy-momentum. It is important to note that the equation of state for every fluid component can be expressed individually according to the Eq. (2.6):

$$p_i = w_i \rho_i. \tag{4.30}$$

4.2.1 Fluid Evolution Equations

The time evolution equations of the proper radial velocity v_i and energy density ρ_i of each individual fluid component stem from the covariant conservation of the energy-momentum tensor ,

$${}^{(4)}\nabla_\mu T_i^{\mu\nu} = 0 \tag{4.31}$$

where i denotes the different fluid components and is not related to the tensor indices. Substituting the energy-momentum tensor, Eq. (4.28), to the conservation

requirement yields to

$$\begin{aligned}(\rho_i + p_i)\left[\left({}^{(4)}\nabla_\mu u_i^\mu\right) u_i^\nu + u_i^\mu {}^{(4)}\nabla_\mu u_i^\nu\right] \\ + {}^{(4)}\nabla_\mu \rho_i u_i^\mu u_i^\mu + {}^{(4)}\nabla_\mu p_i \left(u_i^\mu u_i^\mu + g^{\mu\nu}\right) = 0.\end{aligned} \tag{4.32}$$

For the sake of clarity, the μt components can be calculated first by expanding the covariant derivative with the formula Eq. (A.5) introduced in the Appendix A,

$$\begin{aligned}&(\rho_i + p_i)\left(\partial_t u_i^t + {}^{(4)}\Gamma^t_{tt} u_i^t + {}^{(4)}\Gamma^t_{tr} u_i^r + \partial_r u_i^r + {}^{(4)}\Gamma^r_{rr} u_i^r + 2\partial_\theta u_i^\theta + 2\,{}^{(4)}\Gamma^\theta_{\theta t} u_i^t\right. \\ &\qquad \left. + 2\,{}^{(4)}\Gamma^\theta_{\theta r} u_i^r\right) u_i^t \\ &+ \left(\partial_r \rho_i + \partial_r p_i\right) u_i^r u_i^t + (\rho_i + p_i)\, u_i^t \left(\partial_t u_i^t + {}^{(4)}\Gamma^t_{tt} u_i^t + {}^{(4)}\Gamma^t_{tr} u_i^r\right) + g^{tt}\partial_t p_i \\ &+ \left(\partial_t \rho_i + \partial_t p_i\right) u_i^t u_i^t + (\rho_i + p_i)\, u_i^r \left(\partial_r u_i^t + {}^{(4)}\Gamma^t_{rt} u_i^t + {}^{(4)}\Gamma^t_{rr} u_i^r\right) = 0.\end{aligned} \tag{4.33}$$

The non-zero connection coefficients with respect to the four dimensional metric $g^{\mu\nu}$ can be determined with the formula A.2:

$$\begin{aligned}{}^{(4)}\Gamma^t_{rr} &= H_{rr} H_{rr,t} & {}^{(4)}\Gamma^t_{\theta\theta} &= {}^{(4)}\Gamma^t_{\phi\phi} = H_{\theta\theta} H_{\theta\theta,t}, \\ {}^{(4)}\Gamma^r_{rt} &= \frac{H_{rr,t}}{H_{rr}}, & {}^{(4)}\Gamma^\theta_{\theta t} &= {}^{(4)}\Gamma^\phi_{\phi t} = \frac{H_{\theta\theta,t}}{H_{\theta\theta}}.\end{aligned} \tag{4.34}$$

The other relevant coefficients having the temporal index equal to zero and the coefficients having only spatial indices reduce to the ones calculated earlier in the Eq. (4.11). Substituting the connection coefficients Eq. (4.34), the four-velocity

components Eq. (4.29) and the four dimensional metric components Eq. (4.4) gives

$$\begin{aligned}(\rho_i + p_i)\,\gamma_{v_i}\Bigg[&\gamma_{v_i,t} + \frac{(\gamma_{v_i}v_i)_{,r}}{H_{rr}} - \frac{\gamma_{v_i}v_i H_{rr,r}}{H_{rr}^2} + \frac{\gamma_{v_i}H_{rr,t}}{H_{rr}} + \frac{\gamma_{v_i}v_i H_{rr,r}}{H_{rr}^2} \\ &+2\frac{H_{\theta\theta,t}}{H_{\theta\theta}}\gamma_{v_i} + 2\frac{H_{\theta\theta,r}}{H_{\theta\theta}}\frac{\gamma_{v_i}v_i}{H_{rr}} + \gamma_{v_i,t} \\ &+v_i^2\left(\frac{(\gamma_{v_i}v_i)_{,r}}{H_{rr}} - \frac{\gamma_{v_i}v_i H_{rr,r}}{H_{rr}^2} + \frac{\gamma_{v_i}H_{rr,t}}{H_{rr}}\frac{\gamma_{v_i}v_i H_{rr,r}}{H_{rr}^2}\right)\Bigg] \\ &+ (\rho_i + p_i)_{,r}\,\frac{\gamma_{v_i}v_i}{H_{rr}}\gamma_{v_i} + p_{i,t}\gamma_{v_i}\left(\gamma_{v_i} - \frac{1}{\gamma_{v_i}}\right) + \rho_{i,t}\gamma_{v_i}^2 = 0.\end{aligned} \tag{4.35}$$

Then the correspoding μr components of the conservation of the energy-momentum tensor Eq. (4.32) can be calculated by similar procedure yielding

$$\begin{aligned}&(\rho_i + p_i)\,\frac{\gamma_{v_i}v_i}{H_{rr}}\left(\gamma_{v_i,t} + \frac{(\gamma_{v_i}v_i)_{,r}}{H_{rr}} - \frac{\gamma_{v_i}v_i H_{rr,r}}{H_{rr}^2} + \frac{H_{rr,r}}{H_{rr}}\frac{\gamma_{v_i}v_i}{H_{rr}} + \frac{H_{rr,t}}{H_{rr}}\gamma_{v_i}\right. \\ &\qquad\left. + 2\frac{H_{\theta\theta,t}}{H_{\theta\theta}}\gamma_{v_i} + 2\frac{H_{\theta\theta,r}}{H_{\theta\theta}}\frac{\gamma_{v_i}v_i}{H_{rr}}\right) \\ &+ (\rho_{i,t} + p_{i,t})\,\frac{\gamma_{v_i}^2 v_i}{H_{rr}} + (\rho_{i,r} + p_{i,r})\,\frac{\gamma_{v_i}^2 v_i^2}{H_{rr}^2} \\ &+ (\rho_i + p_i)\left[\gamma_{v_i}\frac{(\gamma_{v_i}v_i)_t}{H_{rr}} + \frac{\gamma_{v_i}v_i}{H_{rr}}\left(\frac{(\gamma_{v_i}v_i)_r}{H_{rr}} + \frac{H_{rr,t}\gamma_{v_i}}{H_{rr}}\right)\right] + p_{i,r}\frac{1}{H_{rr}^2} = 0.\end{aligned} \tag{4.36}$$

First, one can focus on the μt components of the energy-momentum conservation equation, the Eq. (4.35). The first term in the brackets and the third term on the second row can be identified as the temporal component of the expansion scalar Eq. (C.2) introduced in the Appendix C since

$$\gamma_{v_i,t} = \gamma_{v_i}^3 v_i v_{i,t} = \Theta_{Ti}. \tag{4.37}$$

The last four terms on the first row in the Eq. (4.35) as well as the terms on the third row equal to the radial component of the expansion scalar Eq. (C.2) and therefore

$$\frac{(\gamma_{v_i}v_i)_{,r}}{H_{rr}} + \frac{H_{rr,t}}{H_{rr}}\gamma_{v_i} = \frac{\gamma_{v_i}^3 v_{i,r}}{H_{rr}} - \gamma_{v_i}K^r{}_r = \Theta_{Ri}. \tag{4.38}$$

The first equality in Eq. (4.38) requires also the use of the spherically symmetric metric evolution equation, Eq. (4.5). Then, the two terms on the second row in the Eq. (4.35) equal to the angular component of the expansion scalar, Eq. (C.2), again with the help of the spherically symmetric metric evolution equation Eq. (4.5) and the shorthand notation Eq. (4.14):

$$2\frac{H_{\theta\theta,t}}{H_{\theta\theta}}\frac{\gamma_{v_i}}{\alpha}+2\frac{H_{\theta\theta,r}}{H_{\theta\theta}}\frac{\gamma_{v_i}v_i}{H_{rr}}=2\gamma_{v_i}\left(-K^{\theta}{}_{\theta}v_i+\frac{X}{H_{\theta\theta}}\right). \tag{4.39}$$

Now the Eq. (4.35) can be written in terms of the expansion scalar components,

$$\begin{aligned}(\rho_i+p_i)\,\gamma_{v_i}\left[2\Theta_{T_i}+\left(1+v_i^2\right)\Theta_{R_i}+\Theta_{A_i}\right]+(\rho_i+p_i)_{,r}\,\frac{\gamma_{v_i}^2v_i}{H_{rr}}\\ +p_{i,t}\left(\gamma_{v_i}^2-1\right)+\rho_{i,t}\gamma_{v_i}^2=0\end{aligned} \tag{4.40}$$

and then further simplified by using the full expansion scalar Eq. (C.3) as well as the acceleration scalar Eq. (C.8),

$$(\rho_i+p_i)\,\gamma_{v_i}\left(\Theta_i+v_ia_i\right)+(\rho_i+p_i)_{,r}\,\frac{\gamma_{v_i}^2v_i}{H_{rr}}+p_{i,t}\gamma_{v_i}^2v_i^2+\rho_{i,t}\gamma_{v_i}^2=0. \tag{4.41}$$

Now the focus can be turned to the μr component of the energy-momentum conservation equation, Eq. (4.36). After similar procedure than for the μt component and a multiplication by $H_{rr}v_i$ one can write the Eq. (4.36) to a form

$$(\rho_i+p_i)\,\gamma_{v_i}\left(v_i^2\Theta_i+v_ia_i\right)+(\rho_i+p_i)_{,t}\,\gamma_{v_i}^2v_i^2+p_{i,r}\frac{\gamma_{v_i}^2v_i}{H_{rr}}+\rho_{i,r}\frac{\gamma_{v_i}^2v_i^3}{H_{rr}}=0, \tag{4.42}$$

where the expansion scalar formulae Eq. (C.2), Eq. (C.3), the acceleration scalar Eq. (C.8), the spherically symmetric metric evolution equation Eq. (4.5) and the shorthand notation Eq. (4.14) were used, too.

The difference of the two component sets μt and $\mu r\cdot(H_{rr}v_i)$ of the energy momentum

conservation equation, Eq. (4.41) and Eq. (4.42) is of the form

$$(\rho_i + p_i)\,\gamma_{v_i}\Theta_i\left(1 - v_i^2\right) + \rho_{,t}\gamma_{v_i}^2\left(1 - v_i^2\right) + \rho_{,r}\frac{\gamma_{v_i}^2 v_i}{H_{rr}}\left(1 - v_i^2\right) = 0, \tag{4.43}$$

which can then be multiplied by γ_{v_i} and simplified by the convective derivative Eq. (C.10) to yield

$$\frac{\mathrm{d}}{\mathrm{d}\tau}\rho_i = -\Theta_i\left(\rho_i + p_i\right). \tag{4.44}$$

On the other hand, the conservation equation for the pressure can be derived from the difference of the component sets μt the Eq. (4.41) and $\mu r \cdot ({}^{H_{rr}}/_{v_i})$ (the Eq. (4.42) divided by ${}^{1}/_{v_i^2}$)

$$(\rho_i + p_i)\,\gamma_{v_i}a_i\left(v_i - \frac{1}{v_i}\right) + p_{i,t}\gamma_{v_i}^2\left(v_i^2 - 1\right) + p_{i,r}\frac{\gamma_{v_i}^2 v_i}{H_{rr}}\left(1 - \frac{1}{v_i^2}\right) = 0, \tag{4.45}$$

which, multiplying by $\gamma_{v_i}v_i$ and using the convective derivative Eq. (C.4), yields

$$\frac{\mathrm{d}}{\mathrm{d}\sigma}p_i = -a_i\left(\rho_i + p_i\right). \tag{4.46}$$

The continuity equations Eq. (4.44) and Eq. (4.46) can be then used to work even further and define the evolution equations for the proper radial velocity v_i and energy density ρ_i for each fluid component.

The evolution equation of the velocity of each fluid component can now be derived by starting from the acceleration scalar formula Eq. (C.9) and solving for the convective derivative of the velocity

$$\frac{\mathrm{d}v_i}{\mathrm{d}\tau} = \frac{a_i}{\gamma_{v_i}^2} - \frac{v_i}{\gamma_{v_i}}K^r{}_r. \tag{4.47}$$

Next, one can solve the continuity equation of the fluid pressure Eq. (4.46) for the

acceleration scalar a_i and substitute it into the Eq. (4.47) to get

$$\frac{\mathrm{d}v_i}{\mathrm{d}\tau} = \frac{1}{\gamma_{v_i}^2}\frac{1}{\rho_i + p_i}\frac{\mathrm{d}p_i}{\mathrm{d}\sigma} - \frac{v_i}{\gamma_{v_i}}K^r{}_r. \tag{4.48}$$

Expanding the pressure derivative with the Eq. (C.4) and rearranging some terms as well as using the definitions for the equation of state parameter, the Eq. (4.30) and $(\omega_{i,t})_\rho = {}^{p_{i,t}}/_{\rho_i}$ gives

$$\frac{\mathrm{d}v_i}{\mathrm{d}\tau} = -\frac{v_i}{\gamma_{v_i}}\frac{1}{\rho_i\,(1+\omega_i)}\left[(\omega_{i,t})_\rho\,\rho_i + \frac{p_{i,r}}{v_i H_{rr}}\right] + \frac{v_i}{\gamma_{v_i}}K^r{}_r. \tag{4.49}$$

Now, using the definition for the adiabatic sound speed,

$$c_{si}^2 = \frac{\partial p_i}{\partial \rho_i}, \tag{4.50}$$

the Eq. (4.49) transforms to

$$\frac{\mathrm{d}v_i}{\mathrm{d}\tau} = -\frac{v_i}{\gamma_{v_i}}\frac{1}{\rho_i\,(1+\omega_i)}\left[(\omega_{i,t})_\rho\,\rho_i + c_{si}^2\left(\rho_{i,t} + \frac{\rho_{i,r}}{v_i H_{rr}}\right)\right] + \frac{v_i}{\gamma_{v_i}}K^r{}_r. \tag{4.51}$$

The continuity equation for the energy density components Eq. (4.44) and the expansion scalar Eq. (C.3) can be used to get

$$\frac{\mathrm{d}\rho_i}{\mathrm{d}\tau} = \left[\gamma_{v_i}K - \gamma_{v_i}^2\frac{\mathrm{d}v_i}{\mathrm{d}\sigma} - \frac{\gamma_{v_i}v_i}{H_{rr}}\frac{2H_{\theta\theta,r}}{H_{\theta\theta}}\right](\rho_i + p_i)\,, \tag{4.52}$$

which can be broken into the time and radial derivatives of the energy density ρ_i according to the definition of the convective derivative Eq. (C.10). This procedure gives

$$\rho_{i,t} = -\frac{v_i}{H_{rr}}\rho_{i,r} + \left(K - \gamma_{v_i}\frac{\mathrm{d}v_i}{\mathrm{d}\sigma} - \frac{v_i}{H_{rr}}\frac{2H_{\theta\theta,r}}{H_{\theta\theta}}\right)\rho_i\,(1+\omega_i)\,. \tag{4.53}$$

Now, one can substitute the above equation, the Eq. (4.53), to the equation Eq. (4.51)

which yields a form

$$\begin{aligned}\frac{\mathrm{d}v_i}{\mathrm{d}\tau} - v_i c_{si}^2 \frac{\mathrm{d}v_i}{\mathrm{d}\sigma} =& -\frac{v_i}{\gamma_{v_i}} \frac{1}{\rho_i\left(1+\omega_i\right)} \left(\omega_{i,t}\right)_\rho \rho_i + \frac{v_i^2 c_{si}^2}{\gamma_{v_i}\rho_i\left(1+\omega_i\right)H_{rr}}\rho_{i,r} - \frac{v_i c_{si}^2}{\gamma_{v_i}}K \\ &+ \frac{2v_i^2 c_{si}^2 H_{\theta\theta,r}}{\gamma_{v_i} H_{rr} H_{\theta\theta}} - \frac{c_{si}^2}{\gamma_{vi}\left(1+\omega_i\right)}\frac{1}{H_{rr}}\frac{\rho_{i,r}}{\rho_i} + \frac{v_i}{\gamma_{v_i}}K^r{}_r.\end{aligned} \tag{4.54}$$

This can be solved for the time derivative of the proper radial velocity by using the definitions of the convective derivatives Eq. (C.10) and Eq. (C.4) so

$$\begin{aligned}v_{i,t} =& -\frac{\gamma_{cv_i}^2\gamma_{v_i}v_i}{\gamma_{v_i}H_{rr}\gamma_{c_i}^2}v_{i,r} - \frac{\gamma_{cv_i}^2}{\gamma_{v_i}^2}\frac{1}{\left(1+\omega_i\right)}\left[v_i\left(\omega_{i,t}\right)_\rho + \frac{c_{si}^2}{\gamma_{v_i}^2 H_{rr}}\frac{\rho_{i,r}}{\rho_i}\right] \\ &+ \frac{v_i\gamma_{cv_i}^2}{\gamma_{v_i}^2}\left(K^r{}_r - c_{si}^2 K\right) + \frac{2v_i^2 c_{si}^2 H_{\theta\theta,r}\gamma_{cv_i}^2}{\gamma_{v_i}^2 H_{rr}H_{\theta\theta}},\end{aligned} \tag{4.55}$$

where the new gamma factors are

$$\gamma_{cv_i}^2 = \frac{1}{1-c_{si}^2 v_i^2} \quad \text{and} \quad \gamma_{c_i}^2 = \frac{1}{1-c_{si}^2}. \tag{4.56}$$

The equation for the velocity evolution, Eq. (4.55), can be simplified by few more shorthand notations

$$B_i = \gamma_{cv_i}^2\left[v_i\left(\omega_{i,t}\right)_\rho + \frac{c_{si}^2}{\gamma_{v_i}^2 H_{rr}}\frac{\rho_{i,r}}{\rho_i}\right], \tag{4.57}$$

as well as the Eq. (4.14) to get

$$\boxed{v_{i,t} = \frac{v_i\gamma_{cv_i}^2}{\gamma_{v_i}^2}\left(-\frac{\gamma_{v_i}^2}{\gamma_{c_i}^2 H_{rr}}v_{i,r} + K^r{}_r - c_{si}^2 K + \frac{2v_i c_{si}^2 X}{H_{\theta\theta}}\right) - \frac{1}{\gamma_{v_i}^2\left(1+\omega_i\right)}B_i.} \tag{4.58}$$

This equation is the time evolution equation for the proper radial velocity of the fluid components.

The evolution equation for the energy density of each fluid component can be derived by expanding the convective derivative in the Eq. (4.53) by the Eq. (C.4) and substituting the evolution equation of the velocity component, the Eq. (4.74) to the time derivative of the energy density Eq. (4.53)

$$\begin{aligned}\rho_{i,t} = & \\ & \left\{-\gamma_{v_i}\left[\gamma_{v_i}v_i\left(\frac{v_i\gamma_{cv_i}^2}{\gamma_{v_i}^2}\left(-\frac{\gamma_{v_i}^2 v_{i,r}}{\gamma_{c_i}^2 H_{rr}} + K^r{}_r - c_{si}^2 K + \frac{2v_i c_{si}^2 X}{H_{\theta\theta}}\right) - \frac{B_i}{\gamma_{v_i}^2\left(1+\omega_i\right)}\right)\right.\right. \\ & \left.\left. \quad + \frac{\gamma_{v_i}}{H_{rr}}v_{i,r}\right] - \frac{v_i}{H_{rr}}\frac{2H_{\theta\theta,r}}{H_{\theta\theta}} + K\right\}\rho_i\left(1+\omega_i\right) \\ & - \frac{v_i}{H_{rr}}\rho_{i,r}.\end{aligned} \tag{4.59}$$

Then, rearranging terms and dividing by ρ_i gives

$$\boxed{\begin{aligned}\frac{\rho_{i,t}}{\rho_i} = & -\frac{v_i\rho_{i,r}}{H_{rr}\rho_i} + \left(1+\omega_i\right)\left\{K - \gamma_{cv_i}^2\left(\frac{v_{i,r}}{H_{rr}} + v_i^2\left[K^r{}_r - c_{si}^2 K\right] + \frac{2v_i X}{H_{\theta\theta}}\right)\right\} \\ & + v_i B_i,\end{aligned}} \tag{4.60}$$

which is the evolution equation of the energy density for each fluid component.

4.2.2 Explicit Formulation of the Source Terms

The last task, before the spherically symmetric set of ADM equations is complete, is to formulate explicit spherically symmetric expressions for the source terms ρ, S_i, M_{ij} and $T_{\mu\nu}$. This can be done in the rest frame ($v_i = 0$) and thus the normal vector can be written as

$$n_\mu = g_{\mu\nu}u_{rf}^\nu = (-1, 0, 0, 0). \tag{4.61}$$

The explicit formulation can be started from the energy-momentum tensor Eq. (4.28)

by expressing it in the mixed form

$$T^{\mu}_{\ \sigma} = T^{\mu\nu} g_{\nu\sigma} = \sum_i \left[\left(\rho_i + p_i \right) u_i^{\mu} u_i^{\nu} g_{\nu\sigma} + p_i g^{\mu\nu} g_{\nu\sigma} \right], \tag{4.62}$$

where the diagonal components are

$$\begin{aligned} T^{t}_{\ t} &= \sum_i \left[- \left(\rho_i + p_i \right) \gamma_{v_i}^2 + p_i \right], \\ T^{r}_{\ r} &= \sum_i \left[\left(\rho_i + p_i \right) \gamma_{v_i}^2 v_i^2 + p_i \right], \\ T^{\theta}_{\ \theta} &= \sum_i p_i . \end{aligned} \tag{4.63}$$

Only one off-diagonal component remains unzero and it is of the form

$$T^{t}_{\ r} = H_{rr} \sum_i \left(\rho_i + p_i \right) \gamma_{v_i}^2 v_i . \tag{4.64}$$

The energy density, Eq. (3.17) can be now written with the energy-momentum tensor components Eq. (4.63) as follows

$$\rho = -T^{t}_{\ t} = \sum_i \left[\left(\rho_i + p_i \right) \gamma_{v_i}^2 - p_i \right] \tag{4.65}$$

as can be done for the other shorthand notations in Eq. (3.17) as well

$$\begin{aligned} S_i &= T^{t}_{\ i}, \\ S_{ij} &= T_{ij}. \end{aligned} \tag{4.66}$$

Calculation of the components reveals that only one non-zero component exists being the radial component

$$S_r = H_{rr} \sum_i \left(\rho_i + p_i \right) \gamma_{v_i}^2 v_i . \tag{4.67}$$

Also, the source term $M_{\mu\nu}$ defined by the Eq. (3.19) can be formulated in the rest

frame spherically symmetric coordinates

$$\begin{aligned} M^{r}{}_{r} &= \frac{1}{2}\left(T^{r}{}_{r} - T^{t}{}_{t} - 2T^{\theta}{}_{\theta}\right), \\ M^{\theta}{}_{\theta} &= -\frac{1}{2}\left(T^{r}{}_{r} + T^{t}{}_{t}\right), \end{aligned} \tag{4.68}$$

which can be expanded by use of the energy-momentum tensor components Eq. (4.63) as follows

$$\begin{aligned} M^{r}{}_{r} &= \frac{1}{2}\sum_{i}\left[\rho_i - p_i + 2\left(\rho_i + p_i\right)\gamma_{v_i}^{2} v_i^{2}\right] \\ M^{\theta}{}_{\theta} &= \frac{1}{2}\sum_{i}\left(\rho_i - p_i\right). \end{aligned} \tag{4.69}$$

In summary, the complete set of ADM equations in spherical symmetry:

- Metric evolution equations

$$E_{,t} = (1+2E)\frac{H_{rr}H_{\theta\theta}}{H_{\theta\theta,r}}\frac{\kappa}{2}\left[\sum_{i}\left(\rho_i + p_i\right)\gamma_{v_i}^{2} v_i\right] \tag{4.70}$$

- Extrinsic curvature evolution

$$\begin{aligned} K^{r}{}_{r,t} =& -\frac{2X_{,r}}{H_{rr}H_{\theta\theta}} + K^{r}{}_{r}K^{r}{}_{r} + 2K^{\theta}{}_{\theta}K^{r}{}_{r} \\ & - \kappa\frac{1}{2}\sum_{i}\left[\rho_i - p_i + 2\left(\rho_i + p_i\right)\gamma_{v_i}^{2} v_i^{2}\right] \\ K^{\theta}{}_{\theta,t} =& -\frac{X,r}{H_{rr}H_{\theta\theta}} + \frac{1-X^{2}}{H_{\theta\theta}^{2}} + K^{\theta}{}_{\theta}K^{r}{}_{r} + 2K^{\theta}{}_{\theta}K^{\theta}{}_{\theta} - \kappa\frac{1}{2}\sum_{i}\left(\rho_i - p_i\right) \end{aligned} \tag{4.71}$$

- Hamiltonian constraint equation

$$-\frac{2X_{,r}}{H_{rr}H_{\theta\theta}} - \frac{2E}{H_{\theta\theta}^{2}} - \left(K^{\theta}{}_{\theta}\right)^{2} - 2K^{r}{}_{r}K^{\theta}{}_{\theta} = \kappa\sum_{i}\left[\left(\rho_i + p_i\right)\gamma_{v_i}^{2} - p_i\right] \tag{4.72}$$

- Momentum Constraint equation

$$\frac{H_{\theta\theta,r}}{H_{\theta\theta}}\left(K^{\theta}{}_{\theta}-K^{r}{}_{r}\right)+K^{\theta}{}_{\theta,r}=-\frac{1}{2}\kappa H_{rr}\sum_{i}\left(\rho_{i}+p_{i}\right)\gamma_{v_{i}}^{2}v_{i} \tag{4.73}$$

- Fluid proper radial velocity evolution

$$v_{i,t}=\frac{v_{i}\gamma_{cv_{i}}^{2}}{\gamma_{v_{i}}^{2}}\left(-\frac{\gamma_{v_{i}}^{2}}{\gamma_{c_{i}}^{2}H_{rr}}v_{i,r}+K^{r}{}_{r}-c_{si}^{2}K+\frac{2v_{i}c_{si}^{2}X}{H_{\theta\theta}}\right)-\frac{1}{\gamma_{v_{i}}^{2}\left(1+\omega_{i}\right)}B_{i}. \tag{4.74}$$

- Energy density evolution

$$\begin{aligned}\frac{\rho_{i,t}}{\rho_{i}}=&\left(1+\omega_{i}\right)\left\{K-\gamma_{cv_{i}}^{2}\left(\frac{v_{i,r}}{H_{rr}}+v_{i}^{2}\left[K^{r}{}_{r}-c_{si}^{2}K\right]+\frac{2v_{i}X}{H_{\theta\theta}}\right)\right\}\\&+v_{i}B_{i}-\frac{v_{i}\rho_{i,r}}{H_{rr}\rho_{i}}\end{aligned} \tag{4.75}$$

4.3 The Inclusion of the Inhomogeneity

In order the model to have some physical meaning, the boundary and initial conditions have to be specified to correspond to a particular physical problem. In this section the relevant boundary conditions are introduced first and later the reader is guided through the initial conditions where the initial inhomogeneity is included in the model.

4.3.1 Boundary Conditions

The basic idea is that the wLTB model has to blend in to the standard FLRW universe (a universe having FLRW metric Eq. (2.3)) in such a way that at a specified boundary the wLTB model matches the standard cosmological model, hereafter called the background universe. In this thesis, the LTB bubble boundary works as the boundary and therefore at $r = r_b$ the LTB model has to equal the background solution.

As is already introduced in the section 2 the FLRW metric is of the form

$$\mathrm{d}s^{2}=-\mathrm{d}t^{2}+\frac{\bar{a}^{2}(t)\mathrm{d}r^{2}}{1-kr^{2}}+\bar{a}^{2}(t)r^{2}\left(\mathrm{d}\theta^{2}+\sin^{2}\theta\mathrm{d}\phi^{2}\right) \tag{4.76}$$

that is, the background universe is homogeneous and isotropic. In the Eq. (4.76) the bar denotes background quantities. Now, when comparing the FLRW metric Eq. (4.76) to the spherically symmetric LTB metric Eq. (4.4)

$$\mathrm{d}s^2 = -\alpha^2\mathrm{d}t^2 + H_{rr}^2\mathrm{d}r^2 + H_{\theta\theta}^2\left(\mathrm{d}\theta^2 + \sin^2\theta\mathrm{d}\phi^2\right), \tag{4.77}$$

the boundary conditions for the metric components can be read out when matching the two metrics at the bubble boundary [46],

$$H_{rr}(t, r_b) = \frac{\bar{a}(t)}{1 - kr^2} \quad \text{and} \quad H_{\theta\theta}(t, r_b) = \bar{a}(t)r_b. \tag{4.78}$$

The boundary conditions for the other dynamical variable in the model, the extrinsic curvature tensor, can be written by substituting the metric boundary conditions in Eq. (4.78) to the metric evolution equation Eq. (4.5) which gives

$$K^r{}_r(t,r_b) = K^\theta{}_\theta(t,r_b) = -\bar{H} \tag{4.79}$$

where the background Hubble parameter is identified as $\bar{H} = \frac{\bar{a}_{,t}}{\bar{a}}$.

From the above boundary conditions one can derive the boundary conditions also for the curvature function E by solving the Eq. (4.24) for E and substituting the boundary conditions for the metric components in Eq. (4.78). This gives

$$E(t,r_b) = 0. \tag{4.80}$$

The homogeneity and isotropicity of the background universe restric the multicomponental fluid, too. Isotropic universe requires the fluid to be at rest at early times so the proper peculiar velocity $v_i = 0$. The fluid energy densities have to equal the background fluid densities, as well, and since the background universe is homogeneous, one has

$$\rho_i(t,r_b) = \bar{\rho}_i(t). \tag{4.81}$$

4.3.2 Initial conditions

Now, the values at the boundary of the wLTB model has been determined to match the background FLRW universe but the initial conditions are yet to be specified. In addition, no inhomogeneities have yet been included to the model. In this section the inhomogeneity will be introduced in the formulation of the initial conditions and the goal of the rest of this section is to express all the initial metric and fluid energy density quantities in terms of a function which determines the geometry of the initial inhomogeneity in the model.

To include the inhomogeneities in the model, one assumes the perturbations to be adiabatic, that is, to perturb the energy density to induce inhomogeneities in the spatial curvature. In this case, the perturbations can also be formulated in terms of the effective gravitating mass since it is related to the energy density and thus result in adiabatic perturbations.

Consistent with the synchronous gauge a simultaneous big bang is required, i.e. it is assumed that the big bang happened everywhere at the same time, say $t = 0$.

The relation between the energy density and the effective gravitating mass in the background universe can be derived from the Einstein's field equations, Eq. (2.4), with spherically symmetric metric Eq. (4.4) by assuming that the energy density is formed by a perfect fluid, Eq. (2.8). Identifying the radial component of the metric with the corresponding component in the Schwarzchild metric

$$g_{rr} = \left(1 - \frac{2G\bar{F}_M}{r}\right)^{-1}, \tag{4.82}$$

where G is the gravitational constant and $\bar{F}_M$ is the effective gravitating mass, one can then solve for the mass in the tt component of the Einstein's field equations. This gives

$$\bar{F}_M = \frac{4\pi}{3} H_{\theta\theta}^3 \bar{\rho}_M, \tag{4.83}$$

where $\bar{\rho_M}$ is the energy density of the matter component. The bar denotes a background quantity in all equations. [27]

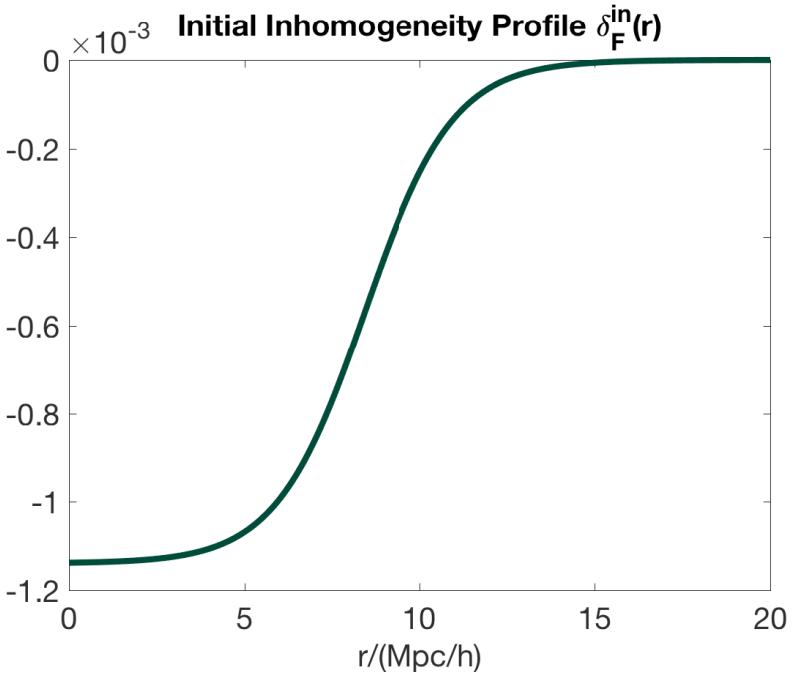

Figure 4.1. An example of an initial inhomogeneity profile when modelling underdensities. The figure is drawn with parameter values $r_0 = {}^{0.25}/_{4} \cdot 100 \cdot 0.674$, $r_{\text{offset}} = r_0$ and $\Delta r = 0.3 r_0$ plugged in the Eq. (4.85) which is then multiplied by the amplitude $\tilde{\delta}_M^{\text{in}} = -1.1 \cdot 10^{-3}$.

Now the initial contrast in the effective gravitating mass can be defined

$$\boxed{\delta_{F_M}^{\text{in}}(r) = \frac{F_M^{\text{in}}}{F_{M,\text{bkg}}^{\text{in}}} - 1 = \hat{\delta}_M^{\text{in}} g_F(r),} \tag{4.84}$$

where $\hat{\delta}_M^{\text{in}}$ describes the amplitude (is just a number) and $g_F(r)$ the initial geometry of the inhomogeneity. The initial inhomogeneity profile is chosen to be of the form

$$\boxed{g_F(r) \equiv \frac{1 - \tanh\left(\frac{r - r_0 - r_{\text{offset}}}{2\Delta r}\right)}{1 + \tanh\left(\frac{r_0}{2\Delta r}\right)},} \tag{4.85}$$

where the parameters r_0 and r_{offset} describe the size and Δr determines the steepness of the inhomogeneity of the effective gravitating mass contrast to the corresponding background quantity. The initial inhomogeneity profile is chosen so that it describes a local underdensity, see the Figure 4.1.

To get the perturbations for each fluid component i, one has to first write the perturbations in terms of the energy densities and then solve for the effective gravitating mass. This has to be done since one cannot exactly divide the effective gravitating mass into fluid components in a sensible way. So, starting from the relation between the effective gravitating mass and the energy density for the matter component Eq. (4.83) one notices that

$$\partial_r F_M^{\text{in}} = 4\pi r^2 \rho_M^{\text{in}}, \tag{4.86}$$

because $H_{\theta\theta}$ is initially directly proportional to the radial component r, as seen in Eq. (4.78). Then, solving the Eq. (4.84) for the effective gravitating mass and differentiating with respect to the radial component r as well as using the two expressions Eq. (4.83) and Eq. (4.86) one can formulate the initial contrast in the energy density for the mass component as follows

$$\delta_{\rho_M}^{\text{in}}(r) = \frac{\rho_M^{\text{in}}}{\bar{\rho}_M^{\text{in}}} - 1 = \hat{\delta}_M^{\text{in}} \left(1 + \frac{r}{3}\partial_r\right) g_F(r). \tag{4.87}$$

Thus, the effective gravitating mass and energy density perturbations are related

$$\delta_{\rho_M}^{\text{in}}(r) = \left(1 + \frac{r}{3}\partial_r\right) \delta_{F_M}^{\text{in}}(r). \tag{4.88}$$

For a general fluid component i one can write the initial density perturbation amplitude in terms of the matter energy density perturbation amplitude as [47]

$$\hat{\delta}_i^{\text{in}} = \hat{\delta}_M^{\text{in}} \left(1 + w_i\right) \frac{5 - 6\bar{c}_{si}^2}{5 - 15\bar{w}_i + 9\bar{c}_{si}^2}. \tag{4.89}$$

The Eq. (4.89) applies only when the perturbation is on superhorizon scales and during matter domination [47]. In practice, this is not a problem in this thesis since the initial conditions are given well before the inhomogeneity scale enters the horizon.

Now, the initial density contrast in energy density for a fluid component i can be

written as

$$\delta^{\rm in}_{\rho_i}(r) = \hat{\delta}^{\rm in}_M\,(1+w_i)\,\frac{5-6\bar{c}^2_{si}}{5-15\bar{w}_i+9\bar{c}^2_{si}}\left(1+\frac{r}{3}\partial_r\right)g_F(r) \tag{4.90}$$

and thus the general form for the effective gravitating mass initial perturbation can be related as

$$\boxed{\delta^{\rm in}_{F_i}(r) = \hat{\delta}^{\rm in}_M\,(1+w_i)\,\frac{5-6\bar{c}^2_{si}}{5-15\bar{w}_i+9\bar{c}^2_{si}}g_F(r).} \tag{4.91}$$

The initial conditions for the peculiar velocities of the fluid components can be all set to zero,

$$\boxed{v^{\rm in}_i = 0} \tag{4.92}$$

because one is assuming an isotropic universe. The initial conditions for the angular metric component can be written straightforwardly as

$$\boxed{H^{\rm in}_{\theta\theta} = \bar{a}^{\rm in} r} \tag{4.93}$$

because of the isotropicity, as well. Remembering the redefinition for the radial metric component Eq. (4.24), the initial conditions can be written by using the above Eq. (4.93)

$$\boxed{H^{\rm in}_{rr} = \frac{\bar{a}^{\rm in}}{\sqrt{1+2E^{\rm in}}}.} \tag{4.94}$$

Remaining components for which the initial conditions needs to be set are the curvature function E as well as the extrinsic curvature tensor components $K^r{}_r$ and $K^\theta{}_\theta$. One can solve the radial component of the extrinsic curvature analytically from the momentum constraint equation Eq. (4.22) (where now $v^{\rm in}_i = 0$)

$$(K^r{}_r)^{\rm in} = \left(K^\theta{}_\theta\right)^{\rm in} + \frac{H^{\rm in}_{\theta\theta}}{H^{\rm in}_{\theta\theta,r}}\left(K^\theta{}_{\theta,r}\right)^{\rm in} \tag{4.95}$$

from where it can be seen that it suffices to determine the initial conditions for the angular component only. For the angular extrinsic curvature tensor component one can formulate the initial conditions by starting from an expression for the effective gravitating total mass given in [46]

$$2GF = \left(\frac{H_{\theta\theta,t}}{H_{\theta\theta}}\right)^2 H_{\theta\theta}^3 - 2EH_{\theta\theta} \tag{4.96}$$

and identifying the extrinsic curvature tensor with the metric evolution equation Eq. (4.5). This gives

$$\left(K^{\theta}_{\ \theta}\right)^2 = \frac{2GF}{H_{\theta\theta}^3} - \frac{2E}{H_{\theta\theta}^2}. \tag{4.97}$$

After some rearranging one can integrate the metric evolution equation for the angular component Eq. (4.5) and use the above equation Eq. (4.97) to write

$$t^{\text{in}} = \int_0^{t_{\text{in}}} \frac{H_{\theta\theta,t}\mathrm{d}t}{H_{\theta\theta}\sqrt{\frac{2GF}{H_{\theta\theta}^3} - \frac{2E}{H_{\theta\theta}^2}}}. \tag{4.98}$$

Since the effective gravitating mass appears here in the integral Eq. (4.98) it is clear why it makes sense to write the inhomogeneities directly in terms of the effective gravitating mass and not the energy density.

Several approximations have to be made in order to be able to integrate the Eq. (4.98) since the effective gravitating mass F and the curvature function E depend on time as well as does the angular metric tensor component $H_{\theta\theta}$.

Approximations can be done if one assumes the initial conditions to be given well after inflation. This yields to a universe where separate causal patches evolve like a corresponding FLRW universe and therefore helps the task of solving the integral in Eq. (4.98). So, first, during the time interval $t < t^{\text{in}}$ the equation of state parameters w_i can be approximated to be constants. Second, if the initial conditions are given early enough the pressure gradients can be approximated to be negligible. Here, the early enough means that inhomogeneities are still outside the horizon. Third, during $t < t^{\text{in}}$ one can set the curvature function $E(t < t^{\text{in}}, r) = E^{\text{in}}$.

With these approximations one can formulate the total effective gravitating mass at

any time in terms of the metric angular components and individual initial effective gravitational masses for all the fluid components as follows

$$F \approx \sum_i \left(\frac{H^{\rm in}_{\theta\theta}}{H_{\theta\theta}}\right)^3 F^{\rm in}_i, \tag{4.99}$$

where Eq. (4.83) for the relation of the effective gravitating mass and energy density as well as the Eq. (4.75) for the evolution of the fluid energy density, on the limit $v_i = 0$ and $H_{rr} \sim H_{\theta\theta}$, were used.

Now, the first term on the right hand side of the Eq. (4.97) can be modified to

$$\frac{2GF}{H^3_{\theta\theta}} \approx \frac{2G}{H^3_{\theta\theta}} \sum_i \left(\frac{H^{\rm in}_{\theta\theta}}{H_{\theta\theta}}\right)^3 F^{{\rm in}_i} = \sum_i \bar{H}^2 \bar{\Omega}^{\rm in}_i \left(1 + \delta^{\rm in}_{F_i}(r)\right) \left(\frac{H^{\rm in}_{\theta\theta}}{H_{\theta\theta}}\right)^3, \tag{4.100}$$

where the equality comes by the virtue of the following equations: the effective gravitating mass initial contrast of Eq. (4.84), the relation between the effective gravitating mass and energy density in Eq. (4.83), the definition of the density parameter in Eq. (2.24), as well as the critical density in Eq. (2.25). Now, one can write the integral in Eq. (4.98) again with the approximation of Eq. (4.100)

$$t^{\rm in} \approx \int_0^{t_{\rm in}} \frac{H_{\theta\theta,t}}{H_{\theta\theta}} \left[\sum_i \bar{H}^2 \bar{\Omega}^{\rm in}_i \left(1 + \delta^{\rm in}_{F_i}(r)\right) \left(\frac{H^{\rm in}_{\theta\theta}}{H_{\theta\theta}}\right)^3 + \frac{2E^{\rm in}}{H^2_{\theta\theta}}\right]^{-\frac{1}{2}} {\rm d}t. \tag{4.101}$$

After some algebra and a variable change $t \to b = {}^{H_{\theta\theta}}/_{H^{\rm in}_{\theta\theta}}$ one can write

$$\bar{H}_{\rm in} t^{\rm in} \approx \int_0^1 \left[\sum_i \bar{\Omega}^{\rm in}_i \left(1 + \delta^{\rm in}_{F_i}(r)\right) b^{-3w_i - 1} + \frac{2E_{\rm in}}{\left(\bar{a}_{\rm in} \bar{H}_{\rm in} r\right)^2}\right]^{-\frac{1}{2}} {\rm d}b. \tag{4.102}$$

By definition, time integrals in a homogeneous FLRW universe are of the form

$$\bar{H}_{\rm in} t^{\rm in} \equiv \int_0^1 \frac{{\rm d}b.}{\sqrt{\sum_i \bar{\Omega}^{\rm in}_i b^{-3w_i - 1}}}. \tag{4.103}$$

Thus, one can relate the perturbation in the effective gravitating mass $\delta^{\rm in}_{F_i}(r)$ and the curvature function E by subtracting the homogeneous case Eq. (4.103) from the

inhomogeneous one Eq. (4.102). This can be easily done if one starts by expanding the right hand side of the integrand in Eq. (4.102) to the first order

$$\frac{1}{\sqrt{\sum_i \bar{\Omega}_i^{\mathrm{in}} b^{-3w_i-1}}}\left[1-\frac{1}{2}\frac{\sum_i \bar{\Omega}_i^{\mathrm{in}}\delta_{F_i}^{\mathrm{in}}(r)b^{-3w_i-1}+\frac{2E_{\mathrm{in}}}{\left(\bar{a}_{\mathrm{in}}\bar{H}_{\mathrm{in}}r\right)^2}}{\sum_i \bar{\Omega}_i^{\mathrm{in}} b^{-3w_i-1}}\right]. \tag{4.104}$$

Now, subtracting the homogeneous time integral Eq. (4.103) from the inhomogeneous one Eq. (4.104) one gets the relation

$$\frac{E_{\mathrm{in}}}{\left(\bar{a}_{\mathrm{in}}\bar{H}_{\mathrm{in}}r\right)^2}\int_0^1 \frac{\mathrm{d}b}{\left(\sum_i \bar{\Omega}_i^{\mathrm{in}} b^{-3w_i-1}\right)^{\frac{3}{2}}} = -\frac{1}{2}\sum_i \bar{\Omega}_i^{\mathrm{in}}\delta_{F_i}^{\mathrm{in}}(r)\int_0^1 \frac{b^{-3w_i-1}\mathrm{d}b}{\left(\sum_i \bar{\Omega}_i^{\mathrm{in}} b^{-3w_i-1}\right)^{\frac{3}{2}}}. \tag{4.105}$$

Since on both sides the integrals remind each other one can define a shorthand notation

$$I_p = \int_0^1 \frac{b^{-p}\mathrm{d}b}{\left(\sum_i \bar{\Omega}_i^{\mathrm{in}} b^{-3w_i-1}\right)^{\frac{3}{2}}}. \tag{4.106}$$

So, one can formulate the initial conditions for the curvature function as follows

$$\frac{E_{\mathrm{in}}}{\left(\bar{a}_{\mathrm{in}}\bar{H}_{\mathrm{in}}r\right)^2} = -\frac{1}{2}\sum_i \bar{\Omega}_i^{\mathrm{in}}\delta_{F_i}^{\mathrm{in}}(r)\frac{I_{3w_i+1}}{I_0}, \tag{4.107}$$

which further can be written in terms of the inhomogeneity profile $g_F(r)$ according to Eq. (4.84)

$$\boxed{\frac{E_{\mathrm{in}}}{\left(\bar{a}_{\mathrm{in}}\bar{H}_{\mathrm{in}}r\right)^2} = -c_E g_F(r),} \tag{4.108}$$

where the constant c_E is of the form

$$c_E = \frac{1}{2}\sum_i^n \bar{\Omega}_i^{\mathrm{in}}\hat{\delta}_i^{\mathrm{in}}\frac{I_{3w_i+1}}{I_0}. \tag{4.109}$$

The last task is to formulate the initial conditions for the extrinsic curvature tensor. Remembering the Eq. (4.97) one can write

$$K^{\theta}_{\ \theta} \approx \bar{H}_{\rm in}\frac{H^{\rm in}_{\theta\theta}}{H_{\theta\theta}}\left[\sum_{i=1}^{n}\bar{\Omega}^{\rm in}_{i}\left(1+\delta^{\rm in}_{F_i}(r)\right)\left(\frac{H^{\rm in}_{\theta\theta}}{H_{\theta\theta}}\right)^{-3w_i-1}+\frac{2E_{\rm in}}{\left(\bar{a}\bar{H}_{\rm in}r\right)^2}\right]^{\frac{1}{2}}, \tag{4.110}$$

and expanding this to first order with small perturbations $\delta^{\rm in}_{F_i}(r)$ one gets

$$\frac{\left(K^{\theta}_{\ \theta}\right)^{\rm in}}{\bar{H}_{\rm in}} = 1+\frac{1}{2}\sum_{i=1}^{n}\bar{\Omega}^{\rm in}_{i}\delta^{\rm in}_{F_i}(r)\left(1-\frac{I_{3w_i+1}}{I_0}\right), \tag{4.111}$$

where the shorthand notation Eq. (4.106) was used. By using the density profile $g_F(r)$ Eq. (4.84), one can define

$$c_K = \frac{1}{2}\sum_{i=1}^{n}\bar{\Omega}^{\rm in}_{i}\bar{\delta}^{\rm in}_{F_i}\left(1-\frac{I_{3w_i+1}}{I_0}\right) \tag{4.112}$$

and finally write

$$\boxed{\frac{\left(K^{\theta}_{\ \theta}\right)^{\rm in}}{\bar{H}_{\rm in}} = 1+c_K g_F(r).} \tag{4.113}$$

Now all the initial conditions for the metric and extrinsic curvature tensor components are written in terms of the density profile $g_F(r)$ which determines the character of the initial inhomogeneity.

4.4 Dimensionless Formulation

It is useful to have the variables and equations in a dimensionless form for the numerical implementation. In this section, the dimensionless formulation of all the necessary parameters and equations for an LTB problem is presented. The LTB parameters are scaled in a way that the results would be more transparent and intuitively interpreted. Then, with the scaled parameters at hand, the necessary equations are written in the dimensionless form.

Considering the boundary conditions for the metric tensor components in Eq. (4.78), one can find a way to scale them as follows

$$\eta_r = \frac{H_{rr}}{\bar{a}} \quad \text{and} \quad \eta_\theta = \frac{H_{\theta\theta}}{\bar{a}r} \tag{4.114}$$

where the bar again means the background quantities. Similarly, one can use the boundary conditions Eq. (4.79) to get the dimensionless form for the extrinsic curvature tensor components,

$$h_i = -\frac{K^i{}_i}{\bar{H}}. \tag{4.115}$$

Evidently, h_i relates the radial and angular relative expansion rates to the background model. This can be seen from the definition of the extrinsic curvature tensor in Eq. (3.5) which contains the first time derivative of the metric tensor components.

The distance from the bubble centre can also be scaled,

$$\tilde{r} = H_0 r, \tag{4.116}$$

as well as the background Hubble parameter

$$\tilde{h} = \frac{\bar{H}}{H_0}, \tag{4.117}$$

with respect to the present-day Hubble parameter value H_0. And as already stated earlier, the radial scale function is replaced by a numerically more stable quantity E, the curvature function. This can also be scaled,

$$e = \frac{E}{\tilde{r}^2}, \tag{4.118}$$

where the Eq. (4.116) and Eq. (4.117) were used. Moreover, for the fluid densities one naturally uses the background density as a scale

$$\Delta_i = \frac{\rho_i}{\bar{\rho}_i}. \tag{4.119}$$

In addition, the time is expressed in terms of a logarithm of the background scale factor

$$y = \log \bar{a} \tag{4.120}$$

which then gives the partial derivative of the form

$$\partial_t = \bar{H}\partial_y. \tag{4.121}$$

4.4.1 Dimensionless Constraint and Evolution Equations

From the dimensionless formulation of the all the necessary LTB parameters defined in the beginning of this section, one can construct dimensionless evolution and constraint equations for the model. This can be done straightforwardly by substituting the dimensionless formulations for the parameters to the spherically symmetric ADM equations already derived earlier.

The momentum constraint equation in the dimensionless form can be formulated by substituting the Eqs. (4.114)–(4.116) and (4.119) to the momentum constraint Eq. (4.73):

$$h_r = h_\theta + \frac{\eta_\theta \tilde{r}}{(\eta_\theta \tilde{r})_{,\tilde{r}}} \left[h_{\theta,\tilde{r}} - \frac{3}{2}\chi_r \sum_i \bar{\Omega}_i \Delta_i \left(1 + w_i\right) \gamma_{v_i}^2 v_i \right], \tag{4.122}$$

where also the formulae for the density parameter Eq. (2.24) and critical density Eq. (2.25) as well as the shorthand notation

$$\chi_i = \bar{a}\tilde{h}\eta_i \tag{4.123}$$

were used.

The Hamiltonian constraint in the dimensionless form can be derived similarly from the Eq. (4.72) by using the formulae in Eqs. (4.114)–(4.119), as well as Eqs. (2.24),

(2.25) and (4.123). This procedure gives

$$h_r = \frac{1}{h_\theta}\left(\frac{\tilde{r}e_{,\tilde{r}} + 2e}{X\chi_r\chi_\theta} + \frac{e}{\chi_\theta^2}\right) - \frac{1}{2}h_\theta + \frac{3}{2h_\theta}\sum_i \bar{\Omega}_i\Delta_i\left(1 + w_i v_i^2\right)\gamma_{v_i}^2. \tag{4.124}$$

* * *

The metric evolution equation for the angular component in Eq. (3.11) can be written in the dimensionless form as

$$\eta_{\theta,y} = \eta_\theta\left(h_\theta - 1\right), \tag{4.125}$$

where the Eqs. (4.114), (4.115) and (4.121) were used. For the radial part, remembering the redefinition in Eq. (4.24), the evolution equation of Eq. (4.70) in a dimensionless scaled form is

$$e_{,y} = \frac{3}{2}\frac{X\chi_\theta}{\tilde{r}}\sum_i \bar{\Omega}_i\Delta_i\left(1 + w_i\right)\gamma_{v_i}^2 v_i, \tag{4.126}$$

where all the above scalings Eqs. (4.114)–(4.121) were used.

With a similar procedure, one can derive the dimensionless evolution equation for the extrinsic curvature tensor, as well. The dimensionless Hamiltonian constraint, Eq. (4.124), can be used to solve for the radial component of the extrinsic curvature tensor appearing in the angular equation, Eq. (4.71). Thus, the angular component of the extrinsic curvature tensor evolution equation in the dimensionless form is

$$h_{\theta,y} = -\frac{3}{2}\left[h_\theta^2 - h_\theta\left(1 + \sum_i \bar{\Omega}_i\bar{w}_i\right) + \sum_i \bar{\Omega}_i\Delta_i\left(v_i^2 + w_i\right)\gamma_i^2\right] + \frac{e}{\chi_\theta^2}. \tag{4.127}$$

In addition, the second Friedmann equation, the so called accelerating Eq. (2.11), was used to convert the time derivative to the partial derivative with respect to the new dimensionless variable y.

The remaining equations to be put in the dimensionless form are the fluid evolution equations. Starting from the fluid proper velocity evolution equation Eq. (4.74) the

dimensionless form can be written as

$$v_{i,y} = \frac{v_i \gamma_{cv_i}^2}{\gamma_{v_i}^2}\left[-\frac{\gamma_{v_i}^2}{\gamma_{c_i}^2 \chi_r} v_{i,\tilde{r}} + h_r^{\mathrm{mc}} + c_{si}^2 h + \frac{2 v_i c_{si}^2 X}{\chi_\theta \tilde{r}}\right] - \frac{1}{1+w_i}\frac{1}{\gamma_{v_i}^2}\tilde{B}_i, \tag{4.128}$$

where

$$\tilde{B}_i = \gamma_{cv_i}\left(v_i (w_{i,y})_\rho + \frac{c_{si}^2}{\gamma_{v_i}^2 \chi_r}\frac{\Delta_{i,\tilde{r}}}{\Delta_i}\right), \tag{4.129}$$

and $h = {}^{(h_r + 2h_\theta)}/_3$. The symbol h_r^{mc} denotes that the radial component of the extrinsic curvature tensor can be analytically solved from the momentum constraint equation, Eq. (4.122).

Then, the dimensionless evolution equation for the fluid energy density components can be derived from the spherically symmetric ADM form Eq. (4.75). Similarly as is done above, one gets

$$\begin{aligned}\Delta_{i,y} =& 3\Delta_i\left\{1 + \bar{w}_i - (1+w_i)\left[h + \frac{1}{3}\gamma_{cv_i}^2\left(\frac{v_{i,\tilde{r}}}{\chi_r} - v_i^2\{h_r^{\mathrm{mc}} - c_{si}h\} + \frac{2Xv_i}{\chi_\theta \tilde{r}}\right)\right]\right\} \\ & - \frac{v_i \Delta_{i,\tilde{r}}}{\chi_r} + v_I \Delta_i \tilde{B}_i.\end{aligned} \tag{4.130}$$

In addition to the scalings, Eqs. (4.114)–(4.121), introduced in this section, the continuity equation Eq. (2.12) is used in the above formulation.

4.4.2 Dimensionless Boundary and Initial conditions

To be complete in the task of formulating the dimensionless set of the spherically symmetric ADM equations, the initial and boundary conditions should be defined, as well. So, starting from the boundary conditions, the dimensionless form on each slice can be written as

$$\eta_\theta(t,r_b) = h_\theta(t,r_b) = \Delta_i(t,r_b) = 1 \quad \text{and} \quad e(t,r_b) = v_i(t,r_b) = 0, \tag{4.131}$$

where the boundary conditions with dimensions, Eqs. (4.78)–(4.81), and the scalings in Eqs. (4.114), (4.115), (4.118) and (4.119) were used. The initial conditions, in turn, are

$$\begin{aligned} \eta_\theta^{\text{in}} &= 1, \quad h_\theta^{\text{in}} = -\left(1 + c_K g_F(r)\right), \\ v_i^{\text{in}} &= 0, \quad \Delta_i^{\text{in}} = 1 + \bar{\delta}_i^{\text{in}} \left(1 + \frac{\tilde{r}}{3}\partial_{\tilde{r}}\right) g_F(r), \end{aligned} \tag{4.132}$$

where initial conditions with dimensions in Eqs. (4.87), (4.92) and (4.93) were used as well as the scalings in Eqs. (4.81), (4.114), (4.115), (4.118) and (4.119).

The initial condition for the radial metric component e requires a little bit more work. In the previous section 4.3.2 initial conditions for the quantity $E_{\text{in}}/\left(\bar{a}_{\text{in}}\bar{H}_{\text{in}}r\right)^2$ was defined in Eq. (4.108). Now, if one applies the dimensionless scaling in Eq. (4.118) one gets

$$e_{\text{in}} = -c_E \left(\bar{a}_{\text{in}} \sqrt{\sum_i \Omega_i \bar{a}_{\text{in}}^{-3(1+w_i)}}\right)^2 g_F(r) \tag{4.133}$$

by using the Friedman equation Eq. (2.9) and the relation between the energy density and the scale factor Eq. (2.27). This completes the task to construct an wLTB model. Results of the model are introduced in the next section .

5 Preliminary Results and a Plan for Statistical Analysis

Now it is time to apply the wLTB model constructed in the previous section 4 to a real world problem. As suggested earlier, the application is the Hubble parameter tension. So, in this section, the wLTB model with a two-component fluid is applied to the Hubble tension problem and preliminary results are introduced. Also, a plan for upcoming statistical analysis is suggested in order for one to get an idea how the results could be compared to observations.

5.1 wLTB with DE and CDM Applied to Hubble Tension

The local and global measurements of the present-day Hubble parameter value H_0 are in tension of about 3.6σ [12, 20]. In this section, a solution with a local underdense LTB bubble is studied. It is expected that a local underdensity would increase the local present-day Hubble parameter value and thus resolve partly or fully the observed tension. In this thesis, the numerical calculations have been performed with a MATLAB program written by Prof. K. Kainulainen.

In the example given in this section, perfect fluid with two components, dark energy (DE) and cold dark matter (CDM) in an LTB universe, is considered in the context of the Hubble tension problem. The input parameter values, such as the dark energy equation of state parameter w_Λ, used in the calculation are introduced in the Table 5.1. These values are plausible examples in the sense of looking for a best example and possible solution.

With the DE + CDM fluid and the input parameter values introduced in the Table 5.1, it is found that the local underdensity indeed increases the local Hubble parameter value. This is demonstrated in the Figure 5.1. Different colours indicate the values at different redshifts, the one coloured with light blue being the present-day ($z = 0$) value.

Table 5.1. The input values for the wLTB model with two-component (DE, CDM) fluid.

Parameter		Input Value	Unit	Reference
Background Hubble constant	$\bar{h}$	0.674	-	[20]
Temperature of the CMB	T	2.725	K	[48]
Physical CDM density parameter	$\Omega_{CDM,0}$	0.26	-	[20]
Dark energy EoS parameter	w_Λ	-1	-	-
Size of the LTB bubble	r_b	$300\bar{h}$	$\mathrm{Mpc}/\bar{h}$	-
Initial amplitude of the inhomogeneity	δ_M	$-1.1 \cdot 10^{-3}$	-	-
Initial position of the bubble wall	r_0	$0.0625 \cdot r_b$	$\mathrm{Mpc}/\bar{h}$	-
Offset in the position	r_{offset}	$0.0625 \cdot r_b$	$\mathrm{Mpc}/\bar{h}$	-
Width of the bubble wall	Δr	$0.3 r_0$	$\mathrm{Mpc}/\bar{h}$	-

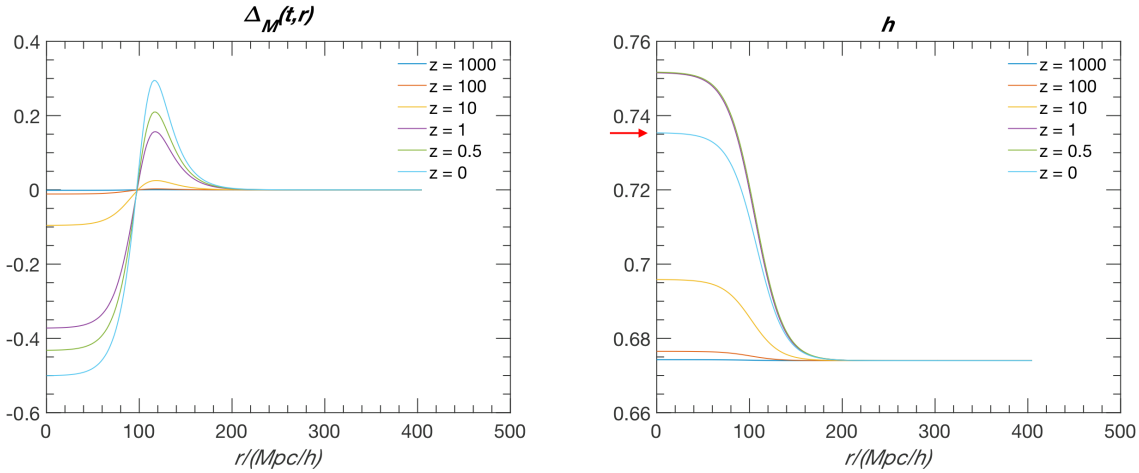

Figure 5.1. In the left panel the energy density contrast for matter (CDM), (Eq. (4.119)) is drawn as a function of the distance calculated from the bubble centre. In the right panel the Hubble parameter is shown as a function of the distance, as well. As can be seen, the underdense bubble increases the local Hubble parameter value towards lower redshifts. The arrow indicates the present-day Hubble parameter value.

It is possible to reach the observed local present-day Hubble parameter value [12]

$$H_0^{\mathrm{local}} = 73.52\,\mathrm{kms}^{-1}\mathrm{Mpc}^{-1}$$

with the wLTB model equipped with the input parameter values shown in the Table 5.1. This is shown in the Figure 5.1 where the $z = 0$ light blue curve reaches the desired magnitude. In the Figure 5.2 and Figure 5.3 surface plots of the energy

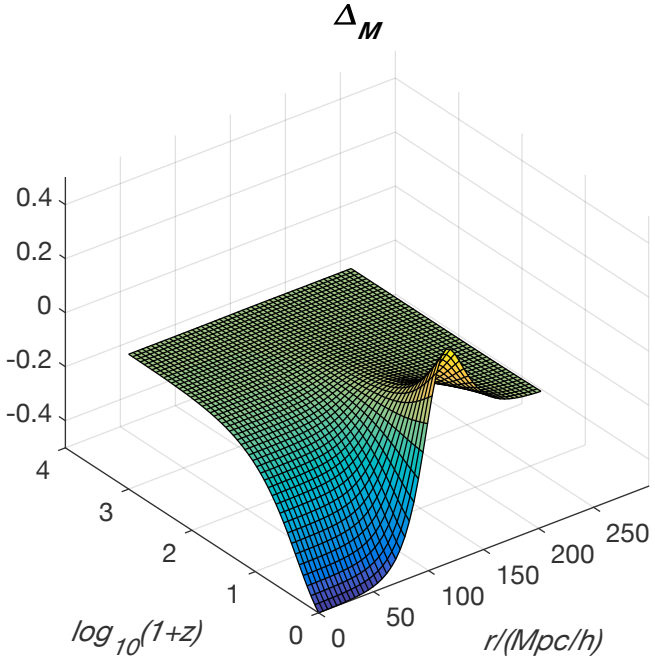

Figure 5.2. The energy density contrast for matter (CDM), (Eq. (4.119)) is plotted as a function of the distance calculated from the bubble centre as well as redshift on a logarithmic scale. See the evolution of the initial inhomogeneity which results in a local underdense bubble.

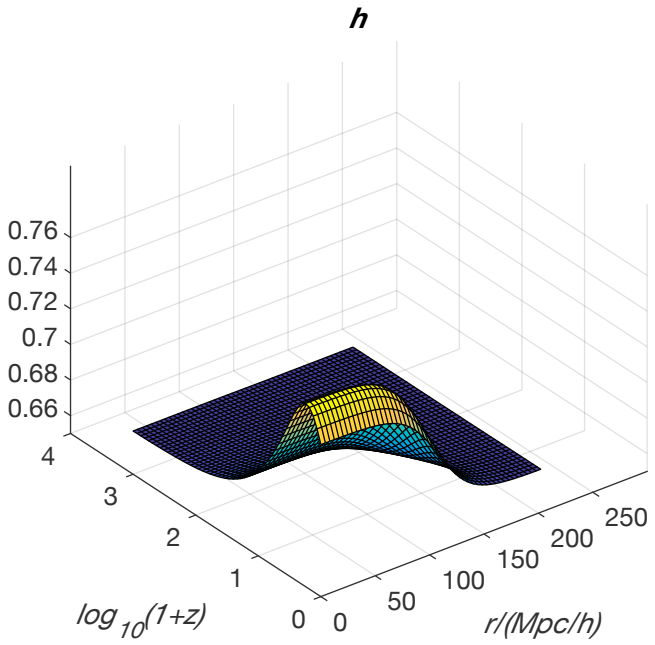

Figure 5.3. The Hubble parameter as a function of distance and redshift on a logarithmic scale. Notice the enhancement towards lower redshifts inside the LTB bubble.

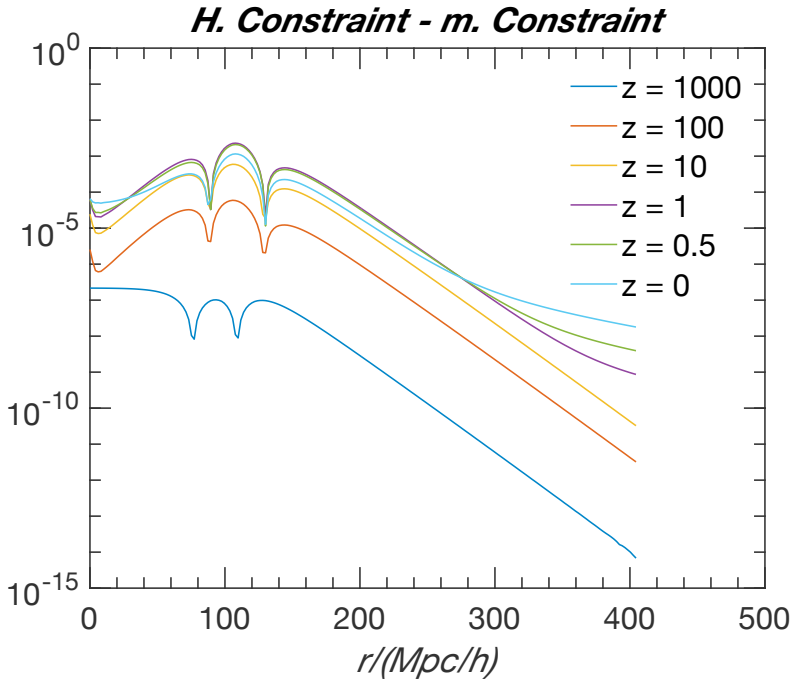

Figure 5.4. The difference of the Hamiltonian constraint and momentum constraint (Eqs. (4.122) and (4.124)) plotted (semilogarithmic) as a function of radius calculated from the bubble centre. Notice how the plots remain well below zero at all redshifts thus indicating sufficient accuracy.

density contrast and Hubble parameter are shown where the same behaviour can be observed. In this example the observer is located in the center of the bubble.

It can be noticed that the Hubble parameter value on redshifts $z = 1$ and $z = 0.5$ is higher than the present-day value $z = 0$. This can be interpreted to be caused by the CDM domination era which ends approximately at $z \approx 0.4$ followed by the dark energy domination.

The numerical accuracy of the calculation can be probed by studying the constraint equations. Figure 5.4 shows the subtraction of the momentum constraint in Eq. (4.122) from the Hamiltonian constraint in Eq. (4.124) as a function of distance from the bubble centre at different fixed redshifts. As can be seen, the constraint values stay well below zero.

The difference calculated at a high redshift $z = 1000$ is of the order 10^{-7}. At later times, i.e. lower redshifts, the difference increases and gets the maximum value of the order of about 10^{-3}. This is still relatively small since all the terms in both of the constraint equations are of the order 10^{0}. This indicates that the accuracy of

the numerical calculation is sufficient.

Studying the Figure 5.4 reveals that the calculation accuracy is highly dependent on the redshift and also decreasing as a function of the distance r calculated from the bubble centre. This can be due to the fact that at earlier times the perturbations are smaller and numerical errors have not had time to grow.

5.2 A Plan: Comparison of Theoretical Results to Observations

In order to get some information out from the theoretical model, one has to be able to compare some parameter values, given by the model, to real world observations. In reality, cosmological observables are, for example redshift and magnitude, and thus the present-day Hubble parameter value cannot be observed directly. To solve this problem, one can formulate all the necessary quantities in terms of the cosmic observables. A way to begin the calculation of the luminosity distance in an LTB universe is shown in the next section. This calculation is a crucial step when comparing theoretical results for example to the supernova data. Later, methods to perform statistical analysis are introduced. This gives the reader an idea how one can compare theoretical results to observations.

5.2.1 Distances in *w*LTB universe

The luminosity distances are needed when the wLTB model is compared to observations. Astronomical data, for example the data from supernovae is highly dependent on the distance. Thus the determination of the luminosity distance in an LTB universe is presented in this section. The next derivation follows the works of [49, 50].

First, one can relate the redshift to the inhomogeneities by considering a radially moving light ray and later relate the redshift to the energy flux of emitted light. This way one gets an expression of the luminosity distance in wLTB model.

A radially moving light ray follows light-like world lines $\mathrm{d}s^2 = 0$ and $\mathrm{d}\theta = \mathrm{d}\phi = 0$ so in a wLTB universe (by using the metric in Eq. (4.4) and the fact that H_{rr} is now

known from the first step of the calculation) one gets

$$\frac{\mathrm{d}t}{\mathrm{d}u} = -H_{rr}\frac{\mathrm{d}r}{\mathrm{d}u}, \tag{5.1}$$

where u is a parametrization of the light-like geodesics and the chosen sign indicates the direction of light, now towards the center of spherical symmetry.

The goal is to relate the time and radial coordinates to the redshift. This can be done by considering a light ray of certain wavelength. Let $\lambda(u)$ be the wavelength of a light ray which is emitted at $t(u)$. Since the length of the signal and the time interval of the full emission equal in natural units one can write that the signal was fully emitted at $t(u) + \lambda(u)$.

Differentiating the tail of the signal $t(u) + \lambda(u)$ with respect to the parameter u gives

$$\frac{\mathrm{d}}{\mathrm{d}u}\left(t(u) + \lambda(u)\right) = -H_{rr}\frac{\mathrm{d}r}{\mathrm{d}u} + \frac{\mathrm{d}\lambda(u)}{\mathrm{d}u}. \tag{5.2}$$

On the other hand, expanding $H_{rr}(t(u) + \lambda(u),r(u)))$ to the first order in λ (if one assumes the signal length $\lambda(u)$ to be small compared to $t(u)$) and then plugging it to the Eq. (5.1) yields

$$\frac{\mathrm{d}}{\mathrm{d}u}\left(t(u) + \lambda(u)\right) = -\frac{\mathrm{d}r}{\mathrm{d}u}\left[H_{rr}(t(u) + \lambda(u),r(u)) + H_{rr,t}(t(u),r(u))\lambda(u)\right]. \tag{5.3}$$

Equating the two expressions, Eqs. (5.2) and (5.3), gives a formula to the light ray length (in first order)

$$\frac{\mathrm{d}\lambda}{\mathrm{d}u} = -\frac{\mathrm{d}r}{\mathrm{d}u}H_{rr,t}(t(u),r(u))\lambda(u). \tag{5.4}$$

This expression can be related to the redshift by differentiating the definition of redshift $z \equiv {}^{(\lambda(u_0) - \lambda(u))}/_{\lambda(u)}$ in terms of the parameter u to get

$$\frac{\mathrm{d}z}{\mathrm{d}u} = -\frac{\mathrm{d}\lambda(u)}{\mathrm{d}u}\frac{\lambda(u_0)}{\lambda^2(u)}, \tag{5.5}$$

and then identifying the Eq. (5.4) and noticing that by definition $\lambda(u_0)/\lambda(u) = z + 1$ yields

$$\frac{\mathrm{d}z}{\mathrm{d}u} = -\frac{\mathrm{d}r}{\mathrm{d}u} H_{rr,t}(t(u),r(u))(1+z). \tag{5.6}$$

Thus the radial component depends on the redshift as follows

$$\frac{\mathrm{d}r}{\mathrm{d}z} = \frac{1}{H_{rr,t}(t,r)(1+z)}. \tag{5.7}$$

For the time coordinate one gets the redshift dependence by using the Eqs. (5.1) and (5.6):

$$\frac{\mathrm{d}t}{\mathrm{d}z} = -\frac{H_{rr}(t,r)}{H_{rr,t}(t,r)(1+z)}. \tag{5.8}$$

Angular distances corresponding to FLRW background universe as perceived by a central observer, can be easily computed from earlier results

$$d_A(z) = H_{\theta\theta}\left(t(z), r(z)\right), \tag{5.9}$$

which approaches

$$\frac{1}{1+z} r(z), \tag{5.10}$$

when the distance r from the bubble centre is much larger than the bubble radius. However, obtaining luminosity distance from the geodesic motions is more complicated and the calculation is not to be finished here in this thesis. It will be pursued elsewhere [51].

5.2.2 Chi-Squared (χ^2) Analysis

After constructing a theoretical model it is good to test how compatible it is with observed data. This can be done by including statistical analysis in the research. In this section the Chi-Squared (χ^2) analysis is introduced to give the reader an idea how one can compare relations of different data sets. Later, the likelihood analysis is discussed.

A χ^2 analysis eases the task of comparing two data sets, say theory and observation, to each other. The χ^2 analysis allows one to determine whether the data given by a certain model is distributed as claimed.

For the purposes of this thesis the χ^2 function for a certain variable can be defined as follows

$$\chi^2\left(\{x_i\}\right) = \sum_{i=1}^{n} \frac{\left(x_{i,\,w\mathrm{LTB}} - x_{i,\,\mathrm{obs.data}}\right)^2}{\left(\delta x_{i,\,\mathrm{obs.data}}\right)^2} \tag{5.11}$$

where $x_{i,\,w\mathrm{LTB}}$ denotes the values given by the wLTB model and $x_{i,\,\mathrm{obs.data}}$ experimentally observed values and $\delta x_{i,\,\mathrm{obs.data}}$ their error. Here the set $\{x_{i,\,\mathrm{obs.data}}\}$ can be for example data containing distance modulus (Eq. (2.40)) as a function of redshift observed from supernovae such as the Joint Light-curve Analysis (JLA) catalogue [52].

The χ^2 function Eq. (5.11) can be minimised in order to get a best-fit parameterisation of the theoretical model such as wLTB. In other words, The χ^2 analysis gives a tool to determine which parameters are the best ones in creating the most realistic parametrisation of the model. For instance, it is expected that the DE equation of state parameter w_Λ takes a little larger value than -1. The best-fit model can then be plotted with observed data to demonstrate the analysis. An example of this plotting is given in the Figure 5.5 which is from [53].

It is expected the wLTB model behaves in such a way that the deeper the bubble i.e. the larger contrast in the initial gravitating mass, the steeper is the peak at low redshifts, see the red plot in the Figure 5.5. The rest of the fit will most likely look like the Einstein-de Sitter model (dashed yellow line the Figure 5.5) starting from the top of the assumed peak. Thus, after the χ^2 analysis one gets already an idea whether the wLTB model is able to describe the real universe.

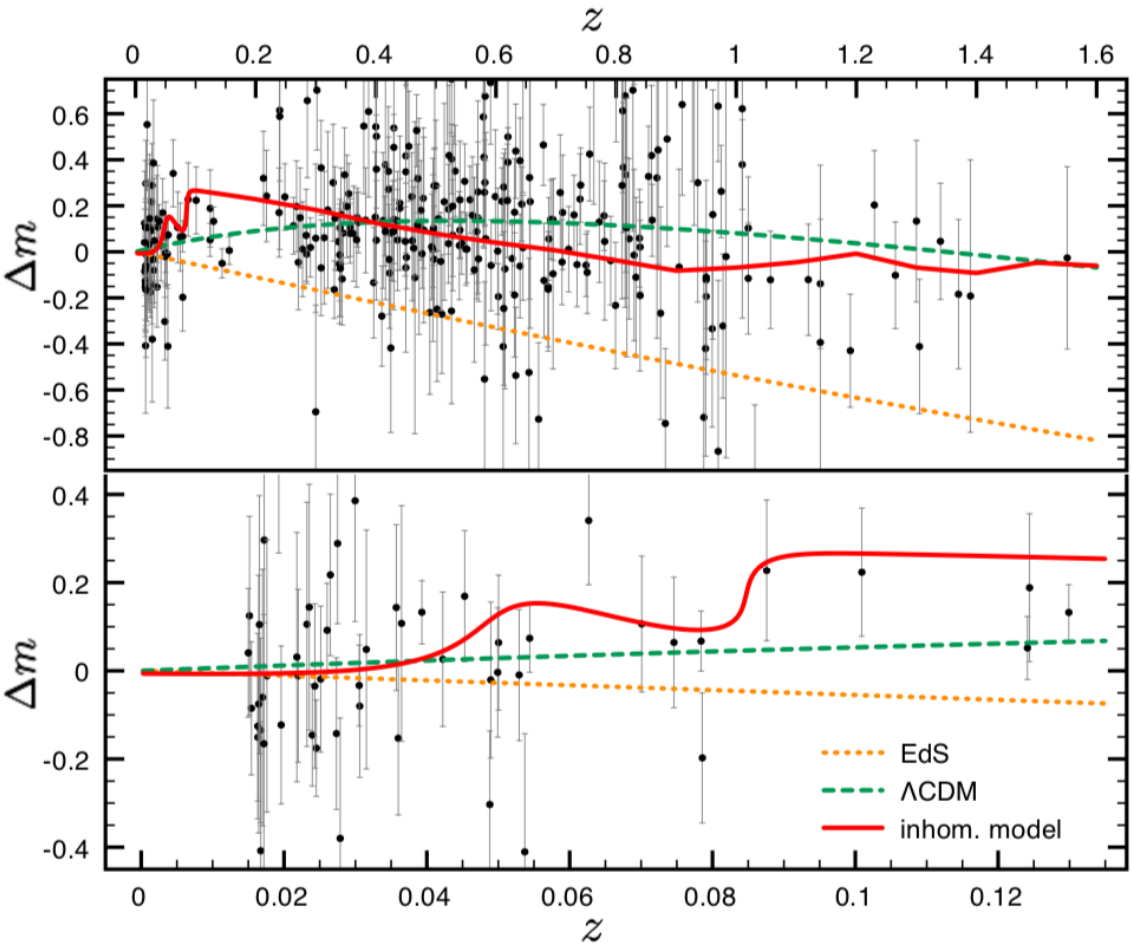

Figure 5.5. In the top panel, the distance modulus Δm with respect to the empty universe for the inhomogeneous model of the paper [53] (red), for the ΛCDM model (dashed green) and for the Einstein-de Sitter model (dashed yellow) together with the full Union Compilation [54] (black binned data) is shown as a function of redshift. In the bottom panel a zoom for low redshifts is presented. This figure is reprinted from [53] with permission of the authors.

5.2.3 Likelihood Analysis

When the χ^2 analysis gives the best parameter values of the model, the likelihood analysis tells how plausible the best-fit parameterisation is compared to the observed data. Thus, one wants to construct a likelihood distribution of the wLTB model with the parameters having the least χ^2 values. This can be done with the following formula

$$L = \left(\prod_i \frac{1}{\delta x_{i,\,\mathrm{obs.data}} \sqrt{2\pi}} \right) e^{-\frac{1}{2}\sum_i \frac{(x_{i,\,w\mathrm{LTB}} - x_{i,\,\mathrm{obs.data}})^2}{(\delta x_{i,\,\mathrm{obs.data}})^2}} \tag{5.12}$$

if the errors $\delta x_{i,\,\mathrm{obs.data}}$ are assumed to be Gaussian. [50]

If the parameter space contains more than two variables, one can marginalise parameters over as follows

$$L = \int \mathrm{d}\mu \prod_i L_i. \tag{5.13}$$

Therefore, it is possible to create contour plots describing the 1σ, $2\sigma, \ldots$ likelihoods of particular parameters.

Performing the statistical analysis would require much computational effort and be beyond the scope of this thesis. Thus, it is left for future studies when the plausibility of the wLTB model can be investigated in terms of the statistical analysis presented in this section.

6 Conclusion

In this thesis the tension between the global and local Hubble parameter measurements is discussed and an alternative model to the Standard Model of Cosmology, the inhomogeneous but spherically symmetric wLTB model, is introduced as a possible candidate for resolving the problem.

The most recent observational results for the Hubble parameter describing the expansion rate of the universe are in tension of about 3.6σ. The local distance ladder method [12] gives a value of $H_0^{\text{local}} = (73{,}52 \pm 1.62)\,\text{kms}^{-1}\text{Mpc}^{-1}$ while the global value derived from the Cosmic Microwave Background radiation data [20] is $H_0^{\text{global}} = (67{,}4 \pm 0.5)\,\text{kms}^{-1}\text{Mpc}^{-1}$. An illustration of these results can be seen in the Figure 1.2 in the section 1.

In this thesis it is assumed that the tension is not caused by unknown systematic errors in the measurements or data analysis but is a result of a local spherically symmetric void. Therefore, an inhomogeneous but spherically symmetric cosmological wLTB model is constructed and used in explaining the phenomenon.

The preliminary results given by the DE + CDM wLTB model with the centred observer predicts that a local underdense region produces higher Hubble parameter values locally. The wLTB model is able to produce the local Hubble parameter measurement with suitably chosen parameters, see Table 5.1. Thus the wLTB model seems to be able to explain the current tension in the expansion rate.

However, final conclusions about the model's compatibility and plausibility in the light of the current observational data cannot be made yet. The statistical analysis and thus the thorough comparison with observations has been left for future investigations. Despite of that, it can be concluded that the model seems to work well, gives reasonable results and the accuracy suffices for current purposes.

In general, the wLTB model presented in this thesis has some challenges. First, the model cannot have arbitrary inhomogeneities and so, in this thesis, the inhomogeneities are restricted to be local and spherically symmetric. This is still an

acceptable approximation for reality, at least qualitatively. However, the Einstein's field equations are very complicated and typically require some symmetry assumptions in order to be solvable, whatsoever.

Second, our location inside the local LTB bubble is restricted. In the analysis of light geodesics in this thesis it is assumed that our location is at the very centre of the void. This ensures that the expansion rate does not vary in terms of direction. In the future, a more general analysis is required by varying our location inside the void. Though, it is probable that our location has to always be somewhere in the vicinity of the bubble centre to avoid the directional differences in the expansion rate.

The Hubble parameter tension is highly topical subject in the science community, currently. Many attempts to solve the tension have been proposed but no other (at the current knowledge) has tried to resolve the problem with wLTB model. ΛLTB or other LTB based models such as [55],[56], [57] in addition to many others have been proposed to alleviate the tension but none has gained general approval. Thus, the wLTB model presented in this thesis is amongst the first models with initially undetermined DE equation of state parameter trying to resolve the Hubble tension. After the statistical analysis, it can be seen how significant the model will be for the Hubble tension research and the cosmology community. The preliminary results obtained in this thesis look encouraging.

In the future, observational experiments will give more information about the nature of the Hubble tension. Thus, it will be important to focus on at least some of the following topics. First, the distance ladder calibrations have to be double-checked in order to conclude whether the Type Ia supernovae are as standard and easily calibrated as they are estimated to be. Second, the behaviour of interstellar gas and dust could be investigated to find out whether they affect the CMB data. Third, if one really wants to rule out the conservative approach, the possibility of systematic errors in the local and global measurements has to be studied. Remembering the history of the Hubble constant measurements, checking the systematic errors may be in order [58].

There are also other ways to determine the present-day Hubble parameter value. For instance, one can measure gravitational-waves emitted by so called standard sirens, which are compact binary systems inspiraling towards a merger. To work out the distance, the waveform of the detected gravitational-waves can be studied. The

recessional velocity of these objects can be determined from the redshift if electromagnetic waves have been observed simultaneously. Thus, combining the distance measurements from the gravitational-wave data and recessional velocity from the corresponding electromagnetic data, one can find the present-day Hubble parameter value. The present-day Hubble parameter value has already been determined by using standard sirens, although the method needs more events to reach the accuracy of the standard candle measurements. On the whole, it will be interesting to see how the gravitational-wave standard siren measurements affect the Hubble tension problem. Currently the error bars [59]

$$H_0^{\mathrm{GW}} = 70.0^{+12.0}_{-8.0}\,\mathrm{kms}^{-1}\mathrm{Mpc}^{-1}$$

are too wide for one to conclude whether they tend to support the CMB or SN Ia regime, let alone resolve the tension.

References

[1] A. Friedmann. Über die Krümmung des Raumes. *Zeitschrift für Physik*, **10**(1):377 – 386, 1922. DOI:10.1007/BF01332580.

[2] A. Friedmann. On the Curvature of Space. *General Relativity and Gravitation*, **31**(12):1991–2000, 1999. DOI: 10.1023/A:1026751225741.

[3] G. Lemaître. Un Univers homogène de masse constante et de rayon croissant rendant compte de la vitesse radiale des nébuleuses extra-galactiques. *Annales de la Société Scientifique de Bruxelles*, **A 47**:49–59, 1927.

[4] G. Lemaître. A Homogeneous Universe of Constant Mass and Increasing Radius accounting for the Radial Velocity of Extra-galactic Nebulae. *Monthly Notices of the Royal Astronomical Society*, **91**(5):483–490, 1931. DOI: 10.1093/mnras/91.5.483.

[5] E. Hubble. A Relation Between Distance and Radial Velocity Among Extra-Galactic Nebulae. *Proceedings of the National Academy of Sciences of the United States of America*, **15**(3):168–173, 1929. DOI: 10.1073/pnas.15.3.168.

[6] A. A. Penzias and R. W. Wilson. A Measurement of Excess Antenna Temperature at 4080 Mc/s. *Astrophysical Journal*, **142**:419–421, 1965. DOI: 10.1086/148307.

[7] R. H. Dicke, P. J. E. Peebles, P. G. Roll, and D. T. Wilkinson. Cosmic Black-Body Radiation. *Astrophysical Journal*, **142**:414–419, 1965. DOI: 10.1086/148306.

[8] W. L. Freedman, B. F. Madore, B. K. Gibson, L. Ferrarese, D. D. Kelson, S. Sakai, et al. Final Results from the Hubble Space Telescope Key Project to Measure the Hubble Constant. *The Astrophysical Journal*, **553**(1):47–72, 2001. DOI: 10.1086/320638.

[9] A. G. Riess, W. Li, P. B. Stetson, A. V. Filippenko, S. Jha, R. P. Kirshner, et al. Cepheid Calibrations from the *Hubble Space Telescope* of the Luminosity of Two Recent Type Ia Supernovae and a Redetermination of the Hubble Constant. *The Astrophysical Journal*, **627**(2):579–607, 2005. DOI: 10.1086/430497.

[10] A. G. Riess, L. Macri, S. Casertano, H. Lampeitl, H. C. Ferguson, A. V. Filippenko, et al. A 3% Solution: Determination of the Hubble Constant with the Hubble Space Telecope and Wide Field Camera 3. *The Astrophysical Journal*, **730**(2):119, 2011. DOI: :10.1088/0004-637X/730/2/119.

[11] A. G. Riess, L. M. Macri, S. L. Hoffmann, D. Scolnic, S. Casertano, A. V. Filippenko, et al. A 2.4% Determination of the Local Value of the Hubble Constant. *The Astrophysical Journal*, **826**(1):56, 2016. DOI: 10.3847/0004-637X/826/1/56.

[12] A. G. Riess, S. Casertano, W. Yuan, L. Macri, B. Bucciarelli, M. G. Lattanzi, et al. Milky Way Cepheid Standards for Measuring Cosmic Distances and Application to *Gaia* DR2: Implications for the Hubble Constant. *The Astrophysical Journal*, **861**(2):126, 2018. DOI: 10.3847/1538-4357/aac82e.

[13] D. N. Spergel, L. Verde, H. V. Peiris, E. Komatsu, M. R. Nolta, C. L. Bennett, et al. First-Year Wilkinson Microwave Anisotropy Probe (WMAP) Observations: Determination of Cosmological Parameters. *The Astrophysical Journal Supplement Series*, **148**(1):175–194, 2003. DOI: 10.1086/377226.

[14] D. N. Spergel, R. Bean, O. Doré, M. R. Nolta, C. L. Bennett, J. Dunkley, et al. Three-Year Wilkinson Microwave Anisotropy Probe (WMAP) Observations: Implications for Cosmology. *The Astrophysical Journal Supplement Series*, **170**(2):377–408, 2007. DOI: 10.1086/513700.

[15] J. Dunkley, E. Komatsu, M. R. Nolta, D. N. Spergel, D. Larson, G. Hinshaw, et al. Five-Year Wilkinson Microwave Anisotropy Probe Observations: Likelihoods and Parameters from The WMAP Data. *The Astrophysical Journal Supplement Series*, **180**(2):306–329, 2009. DOI: 10.1088/0067-0049/180/2/306.

[16] N. Jarosik, C. L. Bennett, J. Dunkley, B. Gold, M. R. Greason, M. Halpern, et al. Seven-year Wilkinson Microwave Anisotropy Probe (WMAP) Observations: Sky Maps, Systematic Errors, and Basic Results. *The Astrophysical Journal Supplement Series*, **192**(2):14, 2011. DOI: 10.1088/0067-0049/192/2/14.

[17] G. Hinshaw, D. Larson, E. Komatsu, D. N. Spergel, C. L. Bennett, J. Dunkley, et al. Nine-year Wilkinson Microwave Anisotropy Probe (WMAP) observations: cosmological parameter results. *The Astrophysical Journal Supplement Series*, **208**(2):19, 2013. DOI: 10.1088/0067-0049/208/2/19.

[18] Planck Collaboration: P. A. R. Ade, N. Aghanim, C. Armitage-Caplan, M. Arnaud, M. Ashdown, F. Atrio-Barandela, et al. Planck 2013 results. XVI. Cosmological parameters. *Astronomy & Astrophysics*, **571**:A16, 2014. DOI: 10.1051/0004-6361/201321591.

[19] Planck Collaboration: P. A. R. Ade, N. Aghanim, M. Arnaud, M. Ashdown, J. Aumont, C. Baccigalupi, et al. Planck 2015 results XIII. Cosmological parameters. *Astronomy & Astrophysics*, **594**:A13, 2016. DOI: 10.1051/0004-6361/201525830.

[20] Planck Collaboration: N. Aghanim, Y. Akrami, M. Ashdown, J. Aumont, C. Baccigalupi, M. Ballardin, et al. Planck 2018 results VI. Cosmological Parameters. *arXiv:1807.06209 [astro-ph.CO]*, 2018.

[21] J. L. Bernal and J. A. Peacock. Conservative Cosmology: Combining Data with Allowance for Unknown Systematics. *Journal of Cosmology and Astroparticle Physics*, **2018**(07):2, 2018. DOI: 10.1088/1475-7516/2018/07/002.

[22] B. Follin and L. Knox. Insensitivity of the Distance Ladder Hubble Constant Determination to Cepheid Calibration Modelling Choices. *Monthly Notices of the Royal Astronomical Society*, **477**(4):4534–4542, 2018. DOI: 10.1093/mnras/sty720.

[23] M. Wyman, D. H. Rudd, R. A.Vanderveld, and W. Hu. Neutrinos Help Reconcile Planck Measurements with the Local Universe. *Physics Review Letters*, **112**:051302, 2014. DOI: 10.1103/PhysRevLett.112.051302.

[24] E. Di Valentino, A. Melchiorri, and J. Silk. Reconciling Planck with the Local Value of H_0 in Extended Parameter Space. *Physics Letters B*, **761**:242 – 246, 2016. DOI: 10.1016/j.physletb.2016.08.043.

[25] Planck Collaboration: P. A. R. Ade, N. Aghanim, M. Arnaud, M. Ashdown, J. Aumont, C. Baccigalupi, et al. Planck 2015 results - XIV. Dark Energy and Modified Gravity. *Astronomy & Astrophysics*, **594**:A14, 2016. DOI: 10.1051/0004-6361/201525814.

[26] V. F. Mukhanov. *Physical Foundations of Cosmology.* Cambridge University Press, 2005.

[27] S. Carroll. *Spacetime and Geometry. An Introduction to General Relativity.* Addison Wesley, 2004.

[28] A. Einstein. Approximative Integration of the Field Equations of Gravitation. *Annalen der Physik*, **49**, 1916.

[29] H. S. Leavitt and E. C. Pickering. Periods of 25 Variable Stars in the Small Magellanic Cloud. *Harvard College Observatory Circular*, **173**:1–3, 1912.

[30] L. Sparke and J. Gallagher. *Galaxies in the Universe: An Introduction.* Cambridge University Press, 2007.

[31] H. Karttunen, P. Kröger, H. Oja, M. Poutanen, and K. J. Donner. *Fundamental Astronomy,* 5th Ed. Springer-Verlag Berlin Heidelberg, 2007.

[32] N. Jackson. The Hubble Constant. *Living Reviews in Relativity*, **18**(1):2, 2015. DOI: 10.1007/lrr-2015-2.

[33] A. Liddle. *An Introduction to Modern Cosmology.* Wiley, 2003.

[34] Particle Data Group: M. Tanabashi, K. Hagiwara, K. Hikasa, K. Nakamura, Y. Sumino, F. Takahashi, et al. Review of Particle Physics. *Physical Review D*, **98**:030001, 2018. DOI: 10.1103/PhysRevD.98.030001.

[35] J. A. Wheeler and K. W. Ford. *Geons, Black Holes and Quantum Foam: A Life in Physics.* W. W. Norton & Company, 1998.

[36] C. W. Misner, K. S. Thorne, and J. A. Wheeler. *Gravitation.* W. H. Freeman and Company, 1973.

[37] R. L. Arnowitt, S. Deser, and C. W. Misner. *Canonical Analysis of General Relativity*, page 127. Warsaw: Polish Scientific Publishers, 1962.

[38] T. W. Baumgarte and S. L. Shapiro. *Numerical Relativity: Solving Einstein's Equations on the Computer.* Cambridge University Press, 2010.

[39] R. M. Wald. *General Relativity.* The University of Chicago Press, 1984.

[40] R. C. Keenan, A. J. Barger, and L. L. Cowie. Evidence for a ~ 300 Megaparsec Scale Under-density in the Local Galaxy Distribution . *The Astrophysical Journal*, **775**(2):62, 2013. DOI:10.1088/0004-637X/775/1/62.

[41] R. B. Tully. More About Clustering on a Scale of 0.1 c. *The Astrophysical Journal*, **323**:1–18, 1987. DOI: 10.1086/165803.

[42] I. Horváth, J. Hakkila, and Z. Bagoly. Possible Structure in the GRB Sky Distribution at Redshift Two. *Astronomy & Astrophysics*, **561**(L12), 2013. DOI: 10.1051/0004-6361/201323020.

[43] G. Lemaître. L'Univers en expansion. *Annales de la Société Scientifique de Bruxelles*, **A 53**:51–85, 1933.

[44] R. C. Tolman. Effect of Inhomogeneity on Cosmological Models. *Proceedings of the National Academy of Sciences of the United States of America*, **20**(3):169–176, 1934. DOI: 10.1073/pnas.20.3.169.

[45] H. Bondi. Spherically Symmetrical Models in General Relativity. *Monthly Notices of the Royal Astronomical Society*, **107**(5-6):410–425, 1947. DOI: 10.1093/mnras/107.5-6.410.

[46] V. Marra and M. Pääkkönen. Exact Spherically-Symmetric Inhomogeneous Model with n Perfect Fluids. *Journal of Cosmology and Astroparticle Physics*, **2012**(1):25, 2012. DOI: 10.1088/1475-7516/2012/01/025.

[47] G. Ballesteros and Julien Lesgourgues. Dark energy with Non-Adiabatic Sound Speed: Initial Conditions and Detectability. *Journal of Cosmology and Astroparticle Physics*, **2010**(10):014, 2010. DOI: 10.1088/1475-7516/2010/10/014.

[48] D. J. Fixsen. The Temperature of the Cosmic Microwave Background. *The Astrophysical Journal*, **707**(2):916–920, 2009. DOI: 10.1088/0004-637X/707/2/916.

[49] K. Enqvist and T. Mattsson. The Effect of Inhomogeneous Expansion on the Supernova Observations. *Journal of Cosmology and Astroparticle Physics*, **2007**(2):19, 2007. DOI: 10.1088/1475-7516/2007/02/019.

[50] M. U. Pääkkönen. LTB Models and Local-Void Scenario. Master's thesis, University of Jyväskylä, Finland, 2010.

[51] K. Kainulainen, V. Marra, and L. Tenhu. In preparation.

[52] Betoule, M., Kessler, R., Guy, J., Mosher, J., Hardin, D., Biswas, R., et al. Improved Cosmological Constraints from a Joint Analysis of the SDSS-II and SNLS Supernova Samples. *Astronomy & Astrophysics*, **568**:A22, 2014. DOI: 10.1051/0004-6361/201423413.

[53] K. Kainulainen and V. Marra. SNe Observations in a Meatball Universe with a Local Void. *Phys. Rev. D*, **80**:127301. DOI: 10.1103/PhysRevD.80.127301.

[54] M. Kowalski, D. Rubin, G. Aldering, R. J. Agostinho, A. Amadon, R. Amanullah, et al. Improved Cosmological Constraints from New, Old, and Combined Supernova Data Sets. *The Astrophysical Journal*, **686**(2):749–778, 2008. DOI: 10.1086/589937.

[55] T. Biswas, A. Notari, and W. Valkenburg. Testing the Void Against Cosmological Data: Fitting CMB, BAO, SN and H_0. *Journal of Cosmology and Astroparticle Physics*, **2010**(11):30, 2010. DOI: 10.1088/1475-7516/2010/11/030.

[56] M. Redlich, K. Bolejko, S. Meyer, G. F. Lewis, and M. Bartelmann. Probing Spatial Homogeneity with LTB Models: a Detailed Discussion. *Astronomy & Astrophysics*, **570**(A63), 2014. DOI: 10.1051/0004-6361/201424553.

[57] M. Tokutake, K. Ichiki, and C. Yoo. Observational Constraint on Spherical Inhomogeneity with CMB and Local Hubble Parameter. *Journal of Cosmology and Astroparticle Physics*, **2018**(03):33, 2018.

[58] V. Trimble. H_0: The Incredible Shrinking Constant 1925-1975. *Publications of the Astronomical Society of the Pacific*, **108**:1073–1082, 1996. DOI: 10.1086/133837.

[59] B. P. Abbott, R. Abbott, T. D. Abbott, F. Acernese, K. Ackley, C. Adams, et al. A Gravitational-wave Standard Siren Measurement of the Hubble Constant. *Nature*, **551**(7678):85–88, 2017. DOI: 10.1038/nature24471.

[60] I. Ciufolini and J. A. Wheeler. *Gravitatation and Inertia*. Princeton University Press, 1995.

Appendices

A Projections of the 4D Riemann tensor to Hypersurfaces

When spacetime is foliated into three spatial and one temporal dimension one has to find a way to relate four-dimensional curvature quantities living on the four-dimensional manifold to three-dimensional spatial quantities living on the three-dimensional hypersurfaces. This means that the four-dimensional Riemann tensor has to be divided into spatial and temporal parts. In this section this is done by executing different projections of the four-dimensional Riemann tensor.

On the four-dimensional manifold, the four-dimensional Riemann curvature tensor is defined as

$$ {}^{(4)}R^{\rho}{}_{\sigma\mu\nu} = \partial_{\mu}\,{}^{(4)}\Gamma^{\rho}{}_{\nu\sigma} - \partial_{\nu}\,{}^{(4)}\Gamma^{\rho}{}_{\mu\sigma} + {}^{(4)}\Gamma^{\rho}{}_{\mu\lambda}\,{}^{(4)}\Gamma^{\lambda}{}_{\nu\sigma} - {}^{(4)}\Gamma^{\rho}{}_{\nu\lambda}\,{}^{(4)}\Gamma^{\lambda}{}_{\mu\sigma}, \tag{A.1} $$

where the four-dimensional Christoffel connection ${}^{(4)}\Gamma^{\sigma}{}_{\mu\nu}$ (metric-compatible and torsion-free) is defined as

$$ {}^{(4)}\Gamma^{\sigma}{}_{\mu\nu} = \frac{1}{2} g^{\sigma\rho} \left(\partial_{\mu} g_{\nu\rho} + \partial_{\nu} g_{\rho\mu} - \partial_{\rho} g_{\mu\nu} \right) \tag{A.2} $$

in terms of the four-dimensional metric of the full manifold $g_{\mu\nu}$ [27]. On the hypersurfaces one can construct the three-dimensional connections ${}^{(3)}\Gamma^{\sigma}{}_{\mu\nu}$ in terms of the spatial metric $h_{\mu\nu}$ and get the three-dimensional Riemann tensor ${}^{(3)}R^{\rho}{}_{\sigma\mu\nu}$ correspondingly [38].

To relate the curvature quantities of different dimensions one has to define a projection tensor. This can be done by raising an index of the spatial metric

$$ h^{\mu}{}_{\nu} = \delta^{\mu}_{\nu} + n^{\mu} n_{\nu}. \tag{A.3} $$

When applied to a tensor, this spatial projection operator i.e. the spatial met-

ric of mixed indices works for every index separately. Therefore for example the three-dimensional covariant derivative of an arbitrary tensor can be constructed by projecting every index of the four-dimensional covariant derivative separately [39]

$$D_\sigma T^{\mu_1\ldots\mu_k}{}_{\nu_1\ldots\nu_l} = h_\sigma{}^\rho \prod_{j=1}^{k} h_{\alpha_j}{}^{\mu_j} \prod_{i=1}^{l} h_{\nu_i}{}^{\beta_i}\, {}^{(4)}\nabla_\rho T^{\alpha_1\ldots\alpha_k}{}_{\beta_1\ldots\beta_l}\,, \tag{A.4}$$

where the four-dimensional covariant derivative is defined in the traditional way [27]

$$\begin{aligned} {}^{(4)}\nabla_\sigma T^{\mu_1\ldots\mu_k}{}_{\nu_1\ldots\nu_l} &= \partial_\sigma T^{\mu_1\ldots\mu_k}{}_{\nu_1\ldots\nu_l} \\ &\quad + \sum_{i=1}^{k} {}^{(4)}\Gamma^{\mu_i}_{\sigma\lambda} T^{\mu_1\ldots\mu_i=\lambda\ldots\mu_k}{}_{\nu_1\ldots\nu_l} \\ &\quad - \sum_{i=1}^{l} {}^{(4)}\Gamma^{\lambda}_{\sigma\nu_i} T^{\mu_1\ldots\mu_k}{}_{\nu_1\ldots\nu_i=\lambda\ldots\nu_l}. \end{aligned} \tag{A.5}$$

Gauss Equation

The four-dimensional Riemann curvature tensor can be related to the three-dimensional spatial metric and the three-dimensional curvature tensor as follows

$${}^{(3)}R_{\mu\nu\rho\sigma} + K_{\mu\rho}K_{\nu\sigma} - K_{\mu\sigma}K_{\rho\nu} = h^\alpha{}_\mu h^\beta{}_\nu h^\gamma{}_\rho h^\delta{}_\sigma\, {}^{(4)}R_{\alpha\beta\gamma\delta}. \tag{A.6}$$

This equation is called Gauss equation and it relates the fully spatially projected four-dimensional Riemann tensor to the extrinsic curvature as well as to the three-dimensional curvature tensor. [39, 38]

The Gauss equation tells that it does not matter whether one performs the differentiation on the whole manifold and then projects it onto a hypersurface or do the differentiation directly on a hypersurface.

For later convenience, one can contract the Gauss equation once by the inverse metric $g^{\rho\mu}$ to get

$${}^{(3)}R_{\nu\sigma} + KK_{\nu\sigma} - K^\rho{}_\sigma K_{\rho\nu} = h^{\alpha\gamma} h^\beta{}_\nu h^\delta{}_\sigma\, {}^{(4)}R_{\alpha\beta\gamma\delta}. \tag{A.7}$$

The second contraction with the expansion of the spatial metric $h^{\mu\nu} = g^{\mu\nu} + n^\mu n^\nu$ yields

$$ {}^{(3)}R + K^2 - K^{\rho\nu}K_{\rho\nu} = {}^{(3)}R + 2n^\alpha n^\gamma {}^{(4)}R_{\alpha\gamma}. \tag{A.8} $$

Codazzi Equation

The four-dimensional Riemann curvature tensor can also be projected in a different way. One can project three of the indices onto the hypersurface and one to the direction of the normal vector i.e. the time direction. This projection relates the extrinsic curvature tensor and the four-dimensional Riemann curvature in a following way

$$ D_\nu K_{\mu\rho} - D_\mu K_{\nu\rho} = h^\alpha{}_\mu h^\beta{}_\nu h^\gamma{}_\rho n^\delta {}^{(4)}R_{\alpha\beta\gamma\delta}. \tag{A.9} $$

This relation is called Codazzi equation. [39, 38]

The Codazzi equation can be contracted and the spatial metric can be expanded to get

$$ D_\nu K_\mu{}^\rho - D_\mu K = -h^\alpha{}_\mu n^\delta {}^{(4)}R_{\alpha\delta}, \tag{A.10} $$

where the minus sign arises from the symmetry properties of the Riemann tensor.

Ricci Equation

The last non-zero projection of the four-dimensional Riemann tensor projects two of the indices to the direction of time and two on the hypersurface. The equation relating this projection is called Ricci equation and it is of the form [38]

$$ \mathcal{L}_{n^\mu} K_{\mu\nu} = n^\sigma n^\rho h^\alpha{}_\mu h^\beta{}_\nu {}^{(4)}R_{\sigma\alpha\rho\beta} - \frac{1}{\alpha} D_\mu D_\nu \alpha - K^\rho{}_\nu K_{\mu\rho}. \tag{A.11} $$

B The Lie Derivative

Differentiation is an operation that describes how fast something is changing. An essential point of taking derivatives is the comparison of objects whose rate of change is under interest. In flat space, it is somewhat easy to compare for example vectors which are located at different points to each other. One can simply move the other vector to the same point without changing its direction or magnitude. In curved space, on the other hand, the transportation is not so straightforward because the result depends on the path taken.

One way to avoid this problem is to find the paths along which an object stays constant. This method is called parallel transportation and is defined by a geometrical structure called connection.

With a connection at hand one can define a covariant derivative which is constructed from a partial derivative and a correction (the connection) to make it tensorial. Thus, the covariant derivative depends on the connection and tells the rate of change along the paths of parallel transportation. So, with a connection one can parallel transport an object to a place where one wants to evaluate it in order to determine the covariant derivative at that point.

The covariant derivative is considered as the generalization of an ordinary partial derivative operator in flat space. Nevertheless, other derivative operations can be defined. If one does not want to define a connection one can use Lie Derivative to differentiate. This means that one has to move the objects by using a different method than parallel transportation.

One can transport tensors also along diffeomorphisms on a manifold. This means that a manifold has invertible maps $\phi : M \to M$ that can be thought to be active coordinate transformations. Because one diffeomorphism takes a point p and maps it to a another point q on the manifold, a one parameter family of diffeomorphisms at a point p forms a curve. [27]

Tensor is an object which takes vectors and dual vectors and produces a multilinear

map to real numbers. Now, it is possible to use the diffeomorphisms to move tensors along the curves of the diffeomorphisms. One can use either the map or its inverse to move tensor forwards or backwards, respectively.

With this property of manifolds one can form a derivative operator and compare the tensors along the flow of diffeomorphisms. From the diffeomorphism point of view the generators are elements of a vector field. Although, normally one thinks that the generators of vector field are the integral curves i.e. the diffeomorphisms. [27]

Now one can form the derivative operator of a tensor by transporting the tensor along the flow of the diffeomorphisms (or vector field, depends on the point of view) and then evaluating the tensor at the point of interest. Thus the Lie derivative is defined

$$\mathcal{L}_V T^{\mu_1 \cdots \mu_k}{}_{\nu_1 \ldots \nu_l}(p) = \lim_{t \to 0} \left[\frac{\Delta_t T^{\mu_1 \cdots \mu_k}{}_{\nu_1 \ldots \nu_l}(p)}{t} \right], \tag{B.1}$$

where V is the vector field along which the comparison of the tensor at different points $\phi(p)$ and p is done. One should notice that the equation Eq. (B.1) can be applied to arbitrary tensors of any rank and the corresponding result is tensor of the same rank, as well. [38]

For later convenience, the Lie derivative of a vector can be written in a simpler way by choosing a convenient coordinate system where the first coordinate is the parameter for the integral curves and the other coordinates can be chosen freely. Then, the generators of the curves can be expressed such that all the others but the first components vanish. With these properties it is possible to force the Lie derivative of an arbitrary vector U^μ along a vector field V^μ to a commutator form called as the Lie Bracket

$$\mathcal{L}_V U^\mu = [V, U]^\mu , \tag{B.2}$$

which is coordinate invariant and therefore applies to any arbitrary vectors in any coordinate system. [27]

One can formulate a similar expression for dual vectors, as well. Considering an arbitrary inner product of a dual vector and a vector one can take the Lie derivative

in two ways. First, one can consider the inner product as a scalar and thus reduce the Lie derivative to a partial derivative. Second, one can use the Leibniz rule to expand the Lie derivative into two parts. Then, these two expressions can be equalized to get a formulation for the Lie derivative of an arbitrary dual vector along a vector field,

$$\mathcal{L}_V \omega_\mu = V^\nu \partial_\nu \omega_\mu + (\partial_\mu V^\mu)\omega_\nu, \tag{B.3}$$

where the symbol ω_μ is an arbitrary dual vector. This expression is independent of coordinate system, as well. [27]

The expressions Eq. (B.2) and Eq. (B.3) can be generalized to a coordinate independent form of the Lie derivative of an arbitrary tensor as follows

$$\begin{aligned}\mathcal{L}_V T^{\mu_1\ldots\mu_k}{}_{\nu_1\ldots\nu_l} = {} & V^\sigma \partial_\sigma T^{\mu_1\ldots\mu_k}{}_{\nu_1\ldots\nu_l} \\ & - \sum_{i=1}^{k} (\partial_\lambda V^{\mu_i}) T^{\mu_1\ldots\lambda=\mu_i\ldots\mu_k}{}_{\nu_1\ldots\nu_l} \\ & + \sum_{i=1}^{l} (\partial_{\nu_i} V^\lambda) T^{\mu_1\ldots\mu_k}{}_{\nu_1\ldots\lambda=\nu_i\ldots\nu_l}.\end{aligned} \tag{B.4}$$

Sometimes it is useful to break the vector field along which the Lie differentiation will be executed to multiple parts. In this case, one has to consider what happens to the Lie derivative. For this purpose, one can use the expression for the Lie derivative of an arbitrary tensor, Eq. (B.4), and write the vector field along which the differentiation is executed as $V^\mu = \alpha n^\mu + \beta^\mu$ which is now, for the sake of an example, divided into normal and tangential parts

$$\begin{aligned}\mathcal{L}_{(\alpha n+\beta)} T^{\mu_1\ldots\mu_k}{}_{\nu_1\ldots\nu_l} = {} & (\alpha n^\sigma + \beta^\sigma) \partial_\sigma T^{\mu_1\ldots\mu_k}{}_{\nu_1\ldots\nu_l} \\ & - \sum_{i=1}^{k} (\partial_\lambda (\alpha n^{\mu_i} + \beta^{\mu_i})) T^{\mu_1\ldots\lambda=\mu_i\ldots\mu_k}{}_{\nu_1\ldots\nu_l} \\ & + \sum_{i=1}^{l} (\partial_{\nu_i} (\alpha n^\lambda + \beta^\lambda)) T^{\mu_1\ldots\mu_k}{}_{\nu_1\ldots\lambda=\nu_i\ldots\nu_l}.\end{aligned} \tag{B.5}$$

Because of the linearity of partial derivatives one can write that

$$\mathcal{L}_{(\alpha n+\beta)} T^{\mu_1 \dots \mu_k}{}_{\nu_1 \dots \nu_l} = \alpha \mathcal{L}_n + \mathcal{L}_\beta. \tag{B.6}$$

C Kinematical Properties of the Fluid Four-Velocity Field

Expansion Scalar

The fractional rate of change of volume expansion for a fluid can be defined as the covariant derivative of the fluid four-velocity [60, 46]

$$\Theta_i = {}^{(4)}\nabla_\mu u_i^\mu, \tag{C.1}$$

where the index i denotes the different fluid components. The quantity Θ_i is called the expansion scalar and it can be divided into temporal, radial and angular components $\Theta_i = \Theta_{T_i} + \Theta_{R_i} + \Theta_{A_i}$ where

$$\begin{aligned}
\Theta_{T_i} &= {}^{(4)}\nabla_t u_i^t = \gamma_{v_i}^3 v_i v_{i,t}, \\
\Theta_{R_i} &= {}^{(4)}\nabla_r u_i^r = \frac{\gamma_{v_i}^3 v_{i,r}}{H_{rr}} - \gamma_{v_i} K^r{}_r, \\
\Theta_{A_i} &= {}^{(4)}\nabla_\theta u_i^\theta + {}^{(4)}\nabla_\phi u_i^\phi = 2\gamma_{v_i}\left(-K^\theta{}_\theta + v_i \frac{X}{H_{\theta\theta}}\right).
\end{aligned} \tag{C.2}$$

The equations for the covariant derivative, Eq. (A.5) in the Appendix A, the connection coefficients, Eqs. (4.11) and (4.34), and the evolution equation of the spherically symmetric metric, Eq. (4.5), as well as the shorthand notation in Eq. (4.14) in the section 4 were used for the latter equalities of every component in the above Eq. (C.2). Thus, the expansion scalar can be written in the form

$$\Theta_i = -\gamma_{v_i} K + \gamma_{v_i}^2 \left(\gamma_{v_i} v_i v_{i,t} + \frac{\gamma_{v_i}}{H_{rr}} v_{i,r}\right) + \frac{\gamma_{v_i} v_i}{H_{rr}} \frac{2H_{\theta\theta,r}}{H_{\theta\theta}}. \tag{C.3}$$

The second term of the Eq. (C.3) gives a motivation to define a convective derivative

as

$$\frac{\mathrm{d}}{\mathrm{d}\sigma} \equiv \gamma_{v_i} v_i \frac{\partial}{\partial t} + \frac{\gamma_{v_i}}{H_{rr}} \frac{\partial}{\partial r} \tag{C.4}$$

so that now, for the expansion scalar one ends up with a formula

$$\Theta_i = -\gamma_{v_i} K + \gamma_{v_i}^2 \frac{\mathrm{d}v_i}{\mathrm{d}\sigma} + \frac{\gamma_{v_i} v_i}{H_{rr}} \frac{2H_{\theta\theta,r}}{H_{\theta\theta}}. \tag{C.5}$$

Acceleration Scalar

The acceleration of the fluid four-velocity field is given by [60, 46]

$$(a_\mu)_i = u_i^\nu {}^{(4)}\nabla_\nu (u_\mu)_i \,, \tag{C.6}$$

which tells the deviation of the geodesic motion of fluid particles. One can also define a scalar quantity

$$a_i = \sqrt{g^{\mu\nu} (a_\mu)_i (a_\nu)_i} \tag{C.7}$$

called acceleration scalar. By using the Eqs. (C.2) and (C.6) one can write the acceleration scalar in the form

$$a_i = \frac{1}{v_i} \Theta_{T_i} + v_i \Theta_{R_i}, \tag{C.8}$$

which, in addition, can be further expanded in terms of the expansion scalar components

$$a_i = \gamma_{v_i}^2 \left(\gamma_{v_i} v_{i,t} + \frac{\gamma_{v_i} v_i}{H_{rr}} v_{i,r} \right) - \gamma_{v_i} v_i K^r{}_r \,. \tag{C.9}$$

The above Eq. (C.9) motivates again for a definition of another convective derivative,

$$\frac{\mathrm{d}}{\mathrm{d}\tau} \equiv \gamma_{v_i} \frac{\partial}{\partial t} + \frac{\gamma_{v_i} v_i}{H_{rr}} \frac{\partial}{\partial r}, \tag{C.10}$$

which, then, yields

$$a_i = \gamma_{v_i}^2 \frac{\mathrm{d}v_i}{\mathrm{d}\tau} - \gamma_{v_i} v_i K^r{}_r. \tag{C.11}$$